JOC The Journal of Organic Chemistry

pubs.acs.org/joc Article

Aggregation and Solvation of Sodium Hexamethyldisilazide: Across the Solvent Spectrum

Ryan A. Woltornist and David B. Collum*

Cite This: J. Org. Chem. 2021, 86, 2406−2422 Read Online

ACCESS | Metrics & More | Article Recommendations | Supporting Information

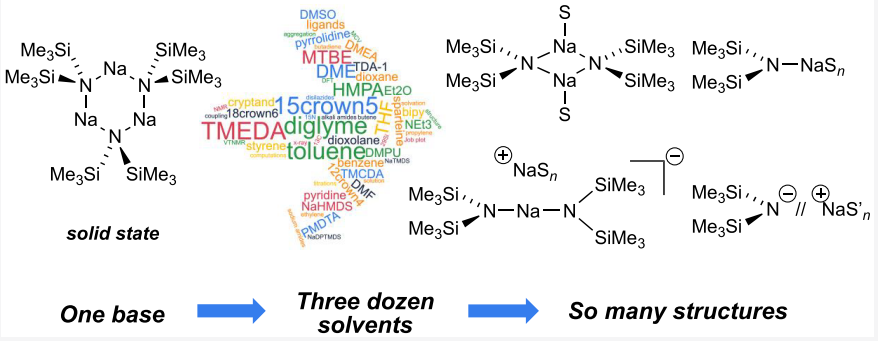

ABSTRACT: We report solution structures of sodium hexamethyldisilazide (NaHMDS) solvated by >30 standard solvents (ligands). These include: toluene, benzene, and styrene; triethylamine and related trialkylamines; pyrrolidine as a representative dialkylamine; dialkylethers including THF, *tert*-butylmethyl ether, and diethyl ether; dipolar ligands such as DMF, HMPA, DMSO, and DMPU; a bifunctional dipolar ligand nonamethylimidodiphosphoramide (NIPA); polyamines *N,N,N′,N′*-tetramethylenediamine (TMEDA), *N,N,N′,N″,N″*-pentamethyldiethylenetriamine (PMDTA), *N,N,N′,N′*-tetramethylcyclohexanediamine (TMCDA), and 2,2′-bipyridine; polyethers 12-crown-4, 15-crown-5, 18-crown-6, and diglyme; 4,7,13,16,21,24-hexaoxa-1,10-diazabicyclo[8.8.8]hexacosane ([2.2.2] cryptand); and tris[2-(2-methoxyethoxy)ethyl]amine (TDA-1). Combinations of ^{1}H, ^{13}C, ^{15}N, and ^{29}Si NMR spectroscopies, the method of continuous variations, X-ray crystallography, and density functional theory (DFT) computations reveal ligand-modulated aggregation to give mixtures of dimers, monomers, triple ions, and ion pairs. ^{15}N−^{29}Si coupling constants distinguish dimers and monomers. Solvation numbers are determined by a combination of solvent titrations, observed free and bound solvent in the slow exchange limit, and DFT computations. The relative abilities of solvents to compete in binary mixtures often match that predicted by conventional wisdom but with some exceptions and evidence of both competitive and cooperative (mixed) solvation. Crystal structures of a NaHMDS cryptate ion pair and a 15-crown-5-solvated monomer are included. Results are compared with those for lithium hexamethyldisilazide, lithium diisopropylamide, and sodium diisopropylamide.

INTRODUCTION

As part of ongoing efforts to pique the community's interest in organosodium chemistry[1] by probing structure−reactivity−selectivity relationships, we have put considerable effort into removing multiple stigmas associated with sodium diisopropylamide (NaDA).[2,3] By contrast, there are no such constraints placed on sodium hexamethyldisilazide (NaHMDS). It is arguably *the* pre-eminent organosodium reagent in both academic and industrial laboratories,[4] finding applications requiring nuanced control of regio-, stereo-, and chemoselectivity.[5] Its solubility, stability, and commercial availability appeal to synthetic chemists and render NaHMDS an attractive target for studying aggregation and solvation. Aside from NaHMDS crystal structures of potential interest to synthetic chemists (Chart 1[6]), there are remarkably few physicochemical studies of NaHMDS in solution.[6d,7−10] Even the computational community has shown little interest.[11]

We describe herein NMR spectroscopic and computational studies of NaHMDS coordinated by several dozen mono-, bi-, and polyfunctional solvents. We use the terms "ligand" and "solvent" interchangeably. Our intention is to establish structural foundations for subsequent studies of solvent-dependent reactivities and selectivities. A secondary but still important goal is to provide a compendium of NaHMDS−solvent combinations to prompt potential consumers to think beyond the standard solvents. Highly solvent-dependent structures offer a potential opportunity for practitioners to

Received: October 26, 2020
Published: January 20, 2021

https://dx.doi.org/10.1021/acs.joc.0c02546
J. Org. Chem. 2021, 86, 2406−2422

Chart 1. X-ray Structures of Homoleptic NaHMDS Aggregates Solvated by Synthetically Standard Solvents[6]

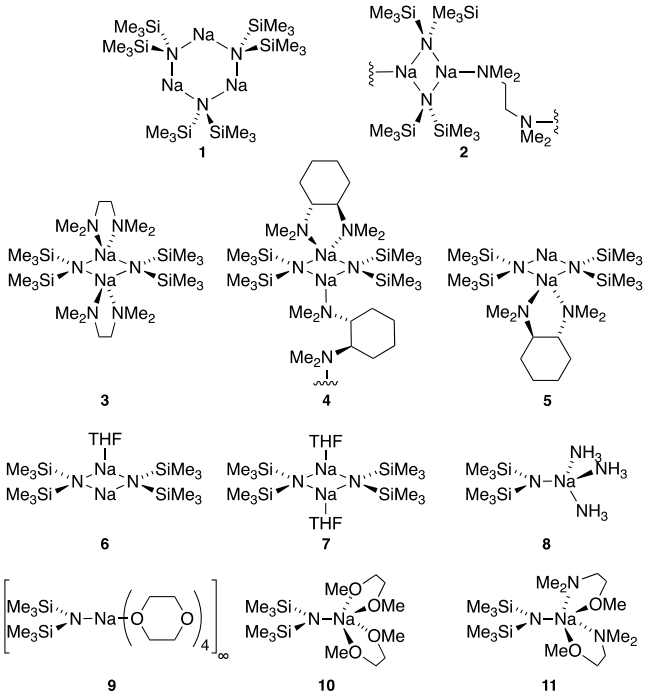

optimize selectivities and reactivities by targeting the underlying structures.[12]

RESULTS AND DISCUSSION

Results from spectroscopic and computational studies are summarized in Table 1 and Chart 2. The lettered entries in Table 1 also designate the coordinated solvent on numbered structures throughout. Dimer **12** and monomer **13** are dominant. Occasionally, dipolar and polydentate solvents at elevated concentrations cause phase separations, the appearance of upfield ^{29}Si resonances as broad mounds, or the complete disappearance of ^{29}Si signals. A chromatographically characterized cryptate ion pair allows us to attribute aberrant spectroscopic behavior to simple ion pairs (**14**). Triple ion **16** is observed in several instances. We observed mixed solvates **15** on many occasions owing to the titration protocols routinely employed, as documented in the Supporting Information; only those observed to the exclusion of homosolvated dimers are included in Table 1. The Supporting Information also includes significant data and pertinent undiscussed observations.

Chart 2. Structural Forms of NaHMDS

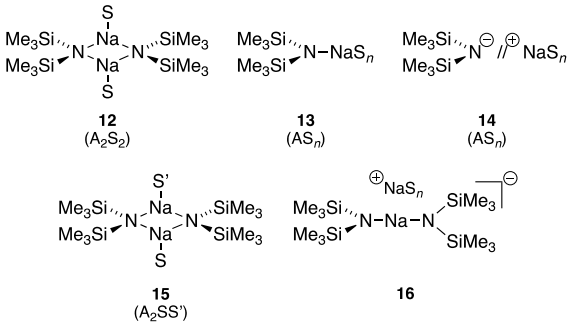

Table 1. Spectroscopic and Computational Data for NaHMDS Dimers and Monomers (12−16, Chart 2) in Different Solvents[a]

entry	solvent	structure (A_mS_n (#))	^{29}Si shifts (ppm ($^1J_{N-Si}$))	solvation energy per S−Na (kcal/mol)
a	toluene	A_2S_2 (**12a**)	−14.4 (7.9)	−1.6
b	benzene	A_2S_2 (**12b**)	−14.2 (7.8)	−2.3
c	styrene	A_2S_2 (**12c**)	−14.3 (7.8)	−1.5
d	DMEA	A_2S_2 (**12d**)	−15.7 (8.7)	−5.9
e	Et_3N	A_2S_2 (**12e**)	−14.5 (7.6)	−4.1
f	*N*-Me-pyrrolidine	A_2S_2 (**12f**)	−15.5 (8.7)	−6.7
g	pyridine	A_2S_2 (**12g**)	−15.4 (8.8)	−7.3
		AS_3 (**13g**)	−20.7 (13.0)	−5.5
h	pyrrolidine	A_2S_2 (**12h**)	−15.5 (9.2)	−8.6
		AS_4 (**13h**)	−19.7 (11.1)	−7.4
i	Et_2O	A_2S_2 (**12i**)	−15.5 (8.3)	−5.0
j	MTBE	A_2S_2 (**12j**)	−15.6 (8.8)	−7.7
k	1,4-dioxane	A_2S_2 (**12k**)	–	−6.5
		AS_3 (**13k**)	–	−6.0
l	1,3-dioxolane	A_2S_2 (**12l**)	−16.0 (8.6)	–
		AS_4 (**13l**)	−21.1 (13.0)	–
m	THF	A_2S_2 (**12m**)	−15.8 (8.7)	−6.7
		AS_4 (**13m**)	−21.7 (13.3)	−5.5
n	HMPA	A_2S_2 (**12n**)	−16.5 (9.8)	−13.6
		AS_3 (**13n**)	−23.7 (13.4)	−11.46
o	DMPU	A_2S_2 (**12o**)	−16.4	−10.9
		AS_2 (**13o**)	−22.5 (13.6)	−13.1
p	DMF	A_2S_4 (**12p**)	–	−8.2
		AS_4 (**13p**)	−22.4 (13.7)	−9.3
q	DMSO	A_2S_4 (**12q**)	–	−6.5
		AS_3 (**13q**)	−20.0 (12.4)	−10.1
r	TMEDA	A_2S_2 (**12r**)	−14.2 (5.8)	−7.4
		AS_2 (**13r**)	−21.0 (11.3)	−9.5
s	(*R*,*R*)-TMCDA	A_2SS' (**15s**)	−15.7 (7.7)	−11.0
			−14.7 (7.1)	
t	(−)-sparteine (**25**)	–	–	–
u	bipy	A_2S (**26u**)	−16.2 (8.8)	–
			−20.5 (12.5)	–
		A_2S_2 (**12u**)	−15.5 (7.8)	−13.2
v	DME	A_2S_2 (**12v**)	−14.8 (7.6)	−9.6
		AS_2 (**13v**)	−21.4 (13.7)	−11.7
w	PMDTA	AS (**13w**)	−22.7 (13.7)	−25.7
x	diglyme	AS (**13x**)	−21.3 (12.7)	−23.4
y	12-crown-4	AS (**13y**)	−22.4 (13.7)	−18.7
z	15-crown-5	AS (**13z**)	−22.1 (13.0)	−29.4
aa	18-crown-6	A_2S (**16aa**)	−22.3 (13.6)	–
		AS (**13aa**)	−21.6 (12.3)	−28.8
bb	TDA-1 (**31**)	A_2S (**16bb**)	−20.5 (13.5)	–
		AS (**13bb**)	−19.7 (12.8)	−23.8
cc	[2.2.2]crypt (**32**)	A_2S (**16cc**)	−20.5 (13.5)	–
		AS (**14cc**)	−27.2	–

[a]Details of the cosolvent and temperatures are found in the Supporting Information.

This paper begins with general discussions of tactics and protocols for studying aggregation and solvation using a few results emblematically. Data are presented only to illustrate the protocols, making no attempt to adjudicate every assignment. General protocols are followed by results from the various mono-, di-, tri-, and polyfunctional solvents (ligands). These assignments are compared to those of lithium hexamethyldi-

https://dx.doi.org/10.1021/acs.joc.0c02546
J. Org. Chem. 2021, 86, 2406−2422

silazide (LiHMDS),[13−15] lithium diisopropylamide (LDA),[13,16] and sodium diisopropylamide (NaDA).[3] We conclude by considering binary mixtures of solvents with studies of relative binding affinities that inadvertently revealed cooperative solvation effects. Computed structures of sodium cations may prove useful in understanding ionizations.

General Methods. NaHMDS, [^{15}N]NaHMDS, sodium tetramethyldisilazide (NaTMDS, **17**)[17] sodium bis(dimethyl(phenyl)silyl)amide (NaDPTMDS, **18**),[18] and sodium disilazide **19**[19] were prepared as white crystalline solids from the disilazanes and sodium metal. The synthesis of $(Me_3Si)_2{}^{15}NH$ has also been reduced from 8 days[20] to 4 h with improved yields. Toluene is used routinely as a cosolvent, but it is *not* an innocent spectator as discussed below. Substitutionally labile *N,N*-dimethylethylamine (DMEA), 2:1 pentane/toluene-d_8, and *tert*-butylmethyl ether (MTBE) were used as cosolvents to record spectra at −120 °C or −110 °C and to optimize solubilities and spectral resolution. No attempt is made to justify or clarify the choice of cosolvent on a case-by-case basis, deferring details to the Supporting Information. ^{1}H, ^{13}C, ^{15}N, and ^{29}Si NMR spectroscopies offered complementary perspectives; ^{13}C and ^{29}Si NMR spectroscopy proved most important.

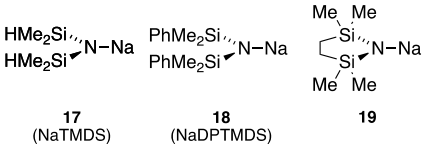

17 (NaTMDS) **18** (NaDPTMDS) **19**

Density functional theory (DFT) computations probe spectroscopically derived structural assignments and experimentally elusive details of solvation. They were carried out at the M06-2X level of theory.[20−22] The standard Def2-SVP basis set was used for geometric optimizations and the expanded Def2-TZVP basis set for single point calculations.[23,24] Prompted by a recent publication revealing consequential free energy changes with larger integration grid sizes,[25] geometric optimizations and single-point calculations employ a refined (99,590) grid. Based on a number of comparisons, the expansion of the grid size has some influence.[26] The molecular solvation events commonplace in alkali amide chemistry require computational procedures that invoke explicit solvation models instead of using an implicit solvation model. Employing both explicit and implicit solvation models can lead to large statistical errors as shown by Houk.[27]

Method of Continuous Variations. The preferences for NaHMDS to form dimers at low solvent loadings and monomers at high solvent loadings (**12** and **13**, Chart 2) are shown using a combination of strategies. The method of continuous variations (MCVs) relies on pairing structurally similar species to afford ensembles of homo- and heteroaggregates that are characteristic of the homoaggregates[28] as illustrated for dimers in eq 1. Heteroaggregates displaying 2:1 and 1:2 stoichiometries characteristic of trimers[29] are *not* observed under any conditions. Monomers observed at elevated ligand concentrations do not heteroassociate.

Pairing partners in MCV are chosen to maximize the NMR spectroscopic resolution while maintaining structural similarity. ^{13}C and ^{29}Si NMR spectroscopies were used to monitor the ensemble in eq 1. ^{1}H NMR spectroscopy was viable but the least effective. ^{15}N NMR spectroscopy using [^{15}N]NaHMDS was supportive but would require both partners be labeled for optimization and was not needed.

NaHMDS and its pairing partners **18** and **19** exist as homodimers in weakly coordinating solvents or at low concentrations of strongly coordinating mono- and difunctional solvents. Results from toluene (Table 1, entry a) illustrate the characterization of dimer ensembles. NaHMDS is insoluble in saturated hydrocarbons but readily dissolves as a 0.10 M solution in 2:1 pentane/toluene at −120 °C. Mixtures of [^{15}N]NaHMDS and NaTMDS contain homodimers **12** and **20** and heterodimer **21** (Figure 1). Heterodimer **21** displays ^{13}C resonances corresponding to the methyl resonances of the TMS and DMS groups in 3:2 proportions, reflecting the number of methyl groups (Figure 1a), a single ^{15}N resonance

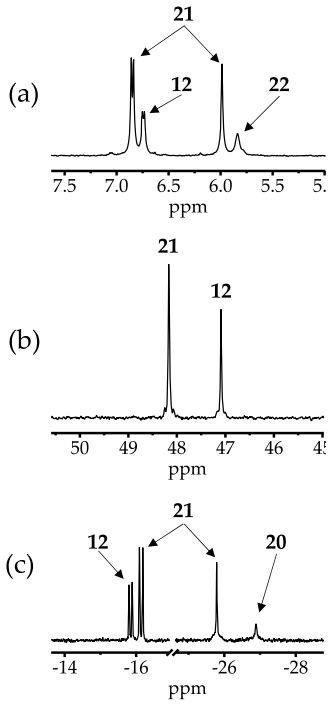

Figure 1. NMR spectra of 1:1 mixtures (0.30 M total titer) of [^{15}N]NaHMDS and NaTMDS (**18**) in 2:1 MTBE/toluene recorded at −80 °C show homo- and heterodimers **12**, **20**, and **21** (eq 1): (a) ^{13}C{^{1}H} NMR (toluene-d_3, 125.79 MHz) spectrum; (b) ^{15}N NMR (toluene-d_3, 60.66 MHz) spectrum; and (c) ^{29}Si NMR (toluene-d_3, 99.36 MHz) spectrum.

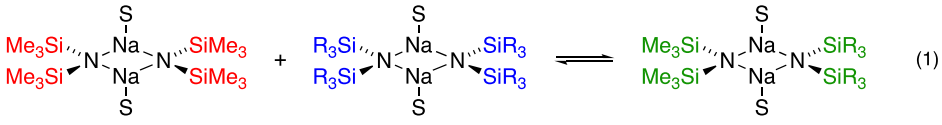

12 **20**; $R_3Si = Me_2HSi$ **22**; $R_3Si = Me_2PhSi$ **21**; $R_3Si = Me_2HSi$ **23**; $R_3Si = Me_2PhSi$

https://dx.doi.org/10.1021/acs.joc.0c02546
J. Org. Chem. 2021, 86, 2406−2422

(Figure 1b), and a pair of ^{29}Si resonances in a 1:1 proportion (Figure 1c). ^{15}N−^{29}Si coupling distinguishes ^{29}Si resonances of the [^{15}N]HMDS and unlabeled TMDS fragments and, more importantly, provides critical structural insights (discussed below).

Plotting the relative concentrations of the homo- and heterodimers versus measured mole fraction[31] of NaHMDS (X_{NaHMDS}) affords a Job plot[30] showing near quantitative heterodimerization (Figure 2). The nonstatistical preference

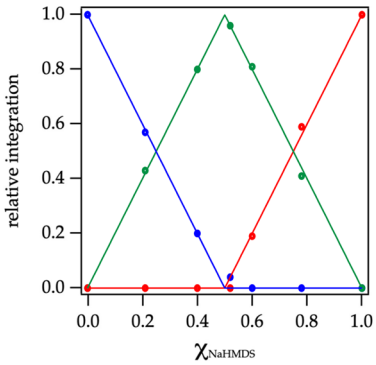

Figure 2. Job plot showing relative integrations of the ^{13}C{^{1}H} resonances of NaHMDS homodimer **12** (red), NaTMDS-derived homodimer **20** (blue), and heterodimer **21** (green; eq 1) versus the measured[29] mole fraction of NaHMDS (X_{NaHMDS}) at 0.30 total molarity[31] in neat toluene at −80 °C. Reprinted from Woltornist, R. A.; Collum, D. B. Using ^{15}N−^{29}Si Scalar Coupling to Determine Aggregation and Solvation States. *J. Am. Chem. Soc.* **2020**, *142*, 6852. Copyright 2020 American Chemical Society.

for heterodimer observed in a number of solvents is supported computationally and presumably derives from relief of congestion in the NaHMDS homodimer **12**. On the other hand, using MTBE/toluene affords a statistical Job plot as shown in Figure 3. The lower preference for heterodimerization can be attributed to a greater solvation energy of the NaHMDS and NaTMDS homodimers, which is supported computationally.

Pairing NaHMDS with the phenyl-containing sodium disilazide **18** unexpectedly favors *homo*dimerization as illustrated in the Job plot in Figure 4. DFT computations of the corresponding homodimer drawn generically as **22** reveal a

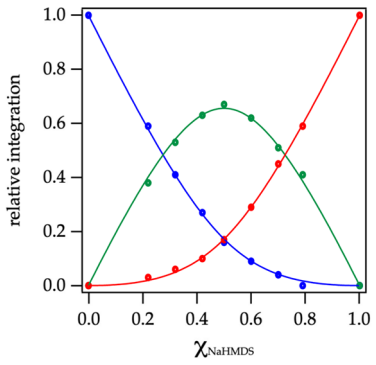

Figure 3. Job plot showing relative integrations of the ^{13}C{^{1}H} resonances of NaHMDS dimer **12** (red), disilazide dimer **20** (blue), and heterodimer **21** (green; eq 1) versus the measured[29] mole fraction of NaHMDS (X_{NaHMDS}) at 0.30 M total molarity in 2:1 MTBE/toluene at −80 °C.

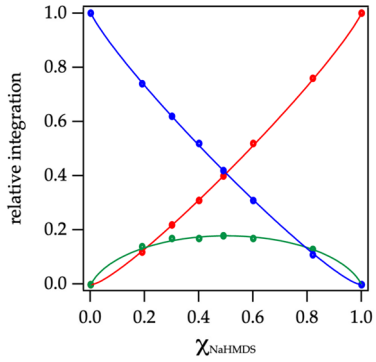

Figure 4. Job plot showing relative integrations of the ^{13}C{^{1}H} resonances of NaHMDS homodimer **12** (red), NaDPTMDS-derived homodimer **22** (blue), and heterodimer **23** (green; eq 1) versus the measured[29] mole fraction of NaHMDS (X_{NaHMDS}) at 0.30 total molarity[31] in neat toluene at −80 °C.

marked canting of the four phenyl moieties toward the sodium nuclei. We attribute this preference for homodimerization to a stabilizing cation−π interaction unique to mixing partner **18**, although this is not confirmed computationally.[34]

Solvent-Dependent Deaggregation. Elevated concentrations of all but the most poorly coordinating solvents cause NaHMDS to deaggregate. Dimer−monomer exchanges are rapid at −80 °C and slow at −120 °C. The clearest view of solvent-concentration-dependent structural changes is derived from HMPA as illustrated in Scheme 1 and Figure 5. The NaHMDS monomers show no associated forms when NaHMDS is mixed with disilazides **18** and **19**, whereas the triple ions **16** form heteroaggregated triple ions.

^{15}N−^{29}Si Scalar Coupling. Figure 5 illustrates coupling that played an unexpectedly important role in the study. In the 1980s, Lukevics and co-workers reported ^{15}N−^{29}Si coupling constants for various disilazanes and several salts.[9] Without the benefits of additional data, they attributed the 7.8 Hz ^{15}N−^{29}Si coupling for NaHMDS in benzene to a ligand-free tetramer, which we are now confident is the benzene-solvated dimer. We find that the ^{15}N−^{29}Si coupling constants correlate with the aggregation state: [^{15}N]NaHMDS-containing homo- and heterodimers display $^{1}J_{N-Si}$ = 7−9 Hz, whereas monomers display $^{1}J_{N-Si}$ = 12−14 Hz (Table 1). The HMPA-solvated ion pair (Table 1, entry m) showed $^{1}J_{N-Si}$ = 16.4 Hz, placing it outside the range of monomers.

The ^{15}N−^{29}Si coupling has the desirable feature that it can be monitored at any temperature, provided that the resonances are not in the midst of coalescing. Figure 6, for example, shows THF-concentration-dependent averaged couplings and ^{29}Si chemical shifts affiliated with NaHMDS deaggregation. The fits attest to the relative solvation numbers of the dimer and monomer. Figure 7 compares the solvent-concentration-dependent coupling for THF and dioxane. The muted tendency of dioxane to deaggregate NaHMDS is evidenced by the intermediate coupling in neat dioxane, indicating ≈50% of the titer corresponds to the dimer.

We habitually use [^{15}N]NaHMDS for all spectroscopic studies as a cross check. The per-sample cost of the label deriving from [^{15}N]NH_4Cl is approximately 7% the price of the NMR tube in which the spectra are recorded.

Titrations. Solvation was studied by titration methods that were recently used for NaDA[3] but have roots in the 1960s alkali metal literature.[35] Serial additions of a coordinating

https://dx.doi.org/10.1021/acs.joc.0c02546
J. Org. Chem. 2021, 86, 2406−2422

Scheme 1. Serial Solvation by HMPA

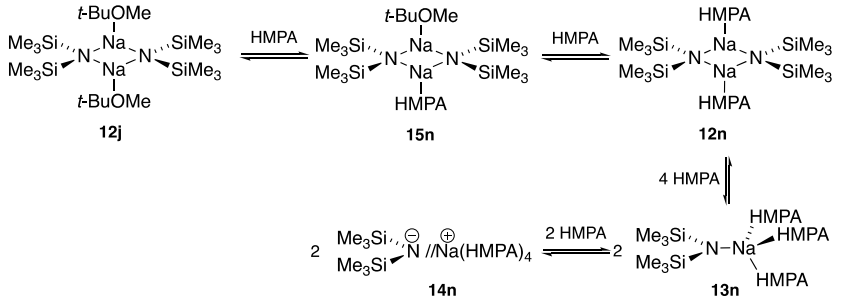

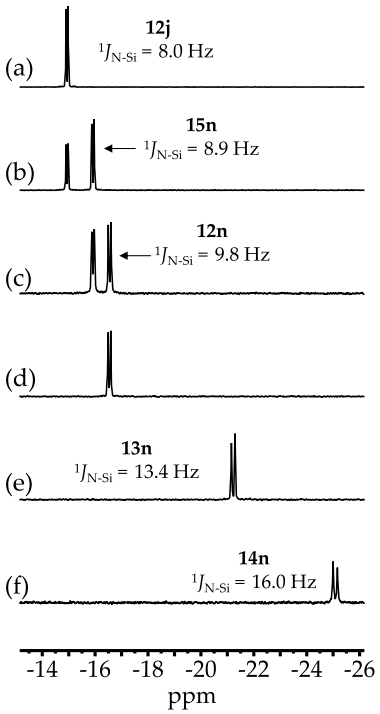

Figure 5. ^{29}Si NMR (various solvents, 99.36 MHz) spectra as follows: (a)−(d) 0.19 M NaHMDS in 2:1 pentane/toluene-d_8 at −120 °C with 0.0 equiv, 0.25 equiv, 0.75 equiv, and 1.0 equiv of HMPA, respectively; (e) 0.10 M NaHMDS in DMEA at −120 °C with 5.0 equiv of HMPA; and (g) 0.10 M NaHMDS in 2:1 HMPA/MTBE recorded at +40 °C (to resolve the coupling).

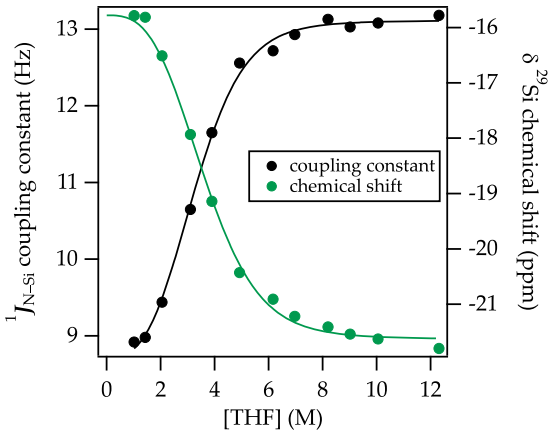

Figure 6. ^{29}Si chemical shift (green) and ^{15}N−^{29}Si coupling constants (black) plotted versus [THF] in 2:1 pentane/toluene as cosolvent measured at −20 °C. The functions are fit to a model based on an A_2S_2−AS_4 equilibrium (Supporting Information). Reprinted from Woltornist, R. A.; Collum, D. B. Using ^{15}N−^{29}Si Scalar Coupling to Determine Aggregation and Solvation States. *J. Am. Chem. Soc.* **2020**, *142*, 6852. Copyright 2020 American Chemical Society.

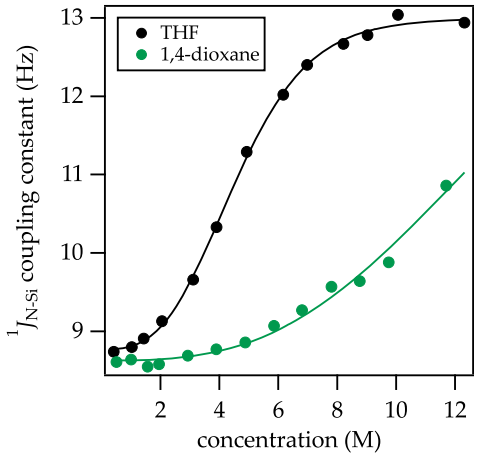

Figure 7. ^{15}N−^{29}Si coupling constants plotted versus [THF] (black) and [1,4-dioxane] (green) in 2:1 pentane/toluene as cosolvent at 20 °C. The functions stem from a model based on an A_2S_2−AS_4 equilibrium (Supporting Information). Reprinted from Woltornist, R. A.; Collum, D. B. Using ^{15}N−^{29}Si Scalar Coupling to Determine Aggregation and Solvation States. *J. Am. Chem. Soc.* **2020**, *142*, 6852. Copyright 2020 American Chemical Society.

solvent to NaHMDS in toluene elicit solvent-concentration-dependent ^{1}H and ^{29}Si chemical shifts of NaHMDS owing to ligand substitution. Figure 8 shows the binding of *N*,*N*,*N*′,*N*″,*N*″-pentamethyldiethylenetriamine (PMDTA). The linearity and sharp end point at 1.0 equiv of PMDTA per sodium attest to the quantitative binding of a single PMDTA per sodium ion. (The structure was subsequently shown to be a monomer as discussed below.) By contrast, weakly coordinating solvents such as Et_3N do not quantitatively displace toluene from the NaHMDS dimer, as evidenced by curvature in the titration (Figure 9). In principle, the details of the curvature attest to the per-sodium solvation number, but such a distinction was not possible. Because of this and the slow exchanges observed at −120 °C, titrations played minor roles. They did, however, serve as an expedient method to monitor the solvent-concentration-dependent structural changes with serial additions through septa (Figure 5).

Solvation in the Slow Exchange Limit. In many cases, homosolvated and mixed-solvated dimers as well as chelated monomers were observed in the limit of slow exchange of free and bound solvent, offering unique probes of solvation numbers and correlated solvation (*vide infra*). Previous studies of LiHMDS show that slow exchange of monodentate solvents

https://dx.doi.org/10.1021/acs.joc.0c02546
J. Org. Chem. 2021, 86, 2406−2422

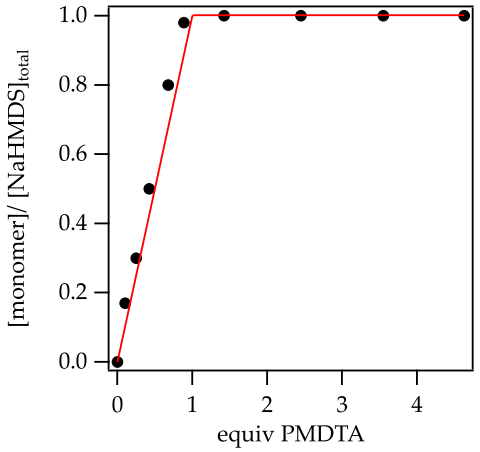

Figure 8. Plot of percent monomer versus equivalents of PMDTA in toluene at −80 °C.

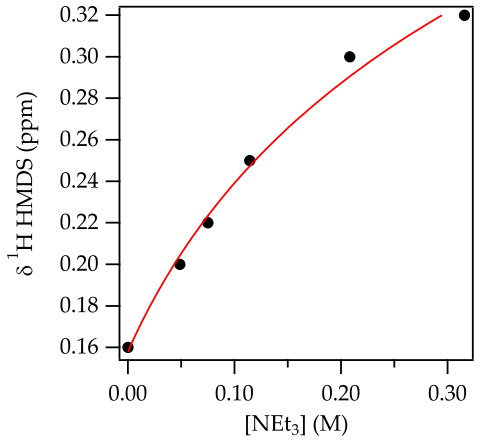

Figure 9. Plot of ^{1}H chemical shifts of NaHMDS versus concentration of Et_3N in neat toluene at −80 °C.[36]

requires the rare combination of high barriers to both associative and dissociative ligand substitutions.[14,37] This slow exchange manifests magnetically distinct ^{29}Si signals for each form as illustrated in the serial titration of NaHMDS with HMPA (Scheme 1 and Figure 5). In some instances, separate ^{13}C signals for free and NaHMDS-bound solvents are observable.

Computed Solvation Numbers. The solvation numbers in Table 1 are derived from both experimental and computational data. The free energies are reported on a solvent-per-sodium basis and benchmarked to their respective unsolvated dimers and monomers (eqs 2 and 3). However, there are

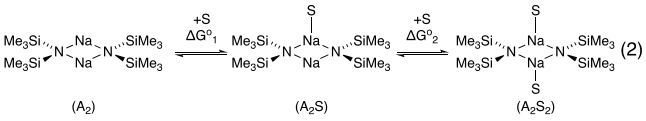

deviations from nonstatistical behavior—so-called "correlated solvation"[38−41]—in which $\Delta G_1 \neq \Delta G_2$ and $\Delta G_3 \neq \Delta G_4$ are prevalent and highly solvent dependent. The hindered bidentate ligand TMEDA, for example, shows ΔG_1 is markedly more negative (favorable) than ΔG_2 (eq 2),[39] and ΔG_3 is more negative than ΔG_4 (eq 3). Similarly, where two or more solvents share a common sodium ion such as AS_2 (eq 3), serial solvation is often correlated: ΔG_3 is more negative than ΔG_4.

Despite such high correlations, Table 1 lists *average* free energies for the multiple solvent−sodium interactions. The separate values for each solvation event are presented in the Supporting Information. Note that the reported free energies in Table 1 do *not* account for denticities. Chelated TMEDA has two sodium−solvent contacts but is considered a single solvent. Thus, ΔG_{TMEDA} is probably most appropriately compared to $2\Delta G_{THF}$.[42] Acutely nonisodesmic[43] comparisons

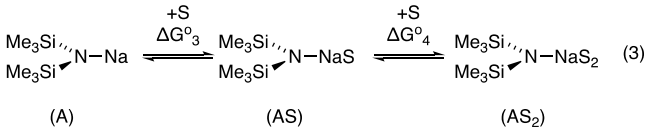

of dimers and monomers (eq 4) are less compelling and mentioned sparingly. Nonetheless, the solvation energies in Table 1, in conjunction with the energy of aggregation of the unsolvated dimer−monomer (eq 5), enable the reader to calculate the solvent-dependent free energies of deaggregations for any solvent directly from the data in Table 1.

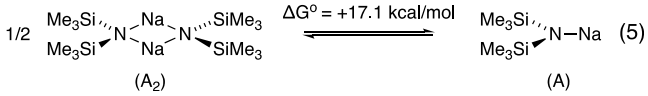

Toluene and Other Hydrocarbons. We now consider observations organized by solvent class with only limited comments about specific protocols. The solubility of NaHMDS in toluene and insolubility in saturated hydrocarbons foreshadowed the formation of an explicitly solvated dimer. Potassium hexamethyldisilazide and sodium triisopropyldisilazide crystallize as dimers bearing η^6 toluene.[44] Many η^6 toluene−sodium complexes[45] and alkali metal−arene π complexes have been characterized crystallographically.[32−34] Spectroscopic evidence suggests toluene binds, albeit weakly, to the LiHMDS dimer[14] and ether- and amine-solvated monomers.[14,15]

Toluene-solvated dimer **12a** was computed to be −0.3 kcal/mol/Na more stable than the crystallographically characterized trimer **1** (Chart 1). Computed serial solvation by toluene (eq 2) is moderately correlated: $\Delta G^0_1 = -2.7$ kcal/mol and $\Delta G^0_2 = -0.5$ kcal/mol (Figure 10). The solvation energy of the corresponding benzene solvate **12b** shows the toluene methyl is *not* a major structural determinant. When titrating toluene solutions of NaHMDS by ethers and amines, one must account for the stabilization by two toluene ligands.

Previous studies showed that arenes, simple alkenes, and internal alkynes weakly bind to the LiHMDS dimer.[14] A survey of potential nontraditional hydrocarbon solvents and cosolvents show that ethylene, propylene, 1-butene, 1-pentene, and 1,3-butadiene failed to measurably dissolve NaHMDS suspended in cyclopentane; the binding energies could be significant but are inadequate to override the lattice energy. Styrene dissolves NaHMDS, probably by forming computa-

https://dx.doi.org/10.1021/acs.joc.0c02546
J. Org. Chem. 2021, 86, 2406−2422

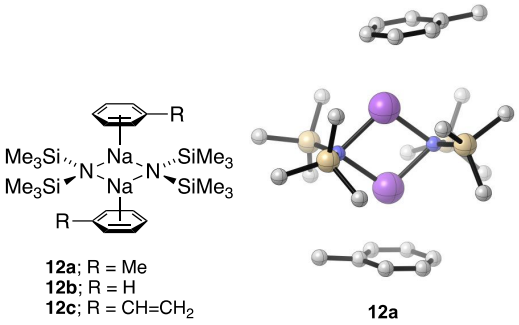

Figure 10. DFT-computed toluene-complexed dimer **12a**.

tionally viable arene complex **12c**, similar to those discussed in the context of anionic polymerizations.[46]

Methylene chloride could be useful and *appears* to interact with NaHMDS in toluene cosolvent at −78 °C, as evidenced by the change in the coupling constant ($^1J_{N-Si}$ = 8.4 Hz relative to $^1J_{N-Si}$ = 7.9 Hz in neat toluene). However, decomposition occurs within 1 h at −40 °C. NaTMDS, by contrast, is soluble *and* stable in CH_2Cl_2 at >−40 °C for >24 h. The relative reactivities of NaHMDS and NaTMDS support the notion that steric congestion increases reactivity through ground-state destabilization and underscores a potential niche for NaTMDS.

Monofunctional Solvents. Monofunctional solvents fall into three approximate categories corresponding to weak, intermediate, and strong solvent donicities[47] as determined by titrations, DFT computations, and inference from experience with LiHMDS and other lithium salts.[14,16]

Weak donors such as Et_2O, MTBE, and trialkylamines (Table 1, entries d−f, i, j) afford disolvated NaHMDS dimers to the exclusion of monomers even in neat donor solvent (eq 6). LiHMDS dimers solvated by sterically demanding and

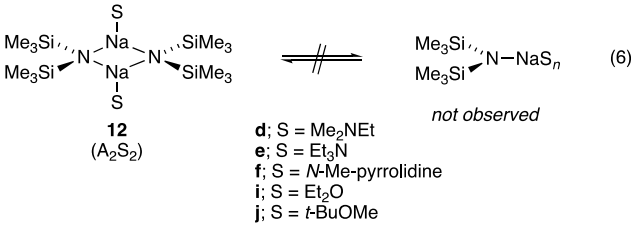

(6)

weakly coordinating[14,48] trialkylamines in toluene are beginning to find synthetic applications,[15] as may NaHMDS−R_3N.[49] The titration of NaHMDS/toluene solutions (Figure 9) shows nonquantitative displacement of toluene by Et_3N (despite computations suggesting it should be quantitative). Although exchange of Et_3N or DMEA was rapid at −120 °C, free and bound *N*-methylpyrrolidine was observed, confirming disolvation. The less congested disolvated NaTMDS homodimer **20** and NaHMDS−NaTMDS heterodimer **21** (eq 1) show disolvation by Et_3N in the slow-exchange limit. Computations clearly support disolvation as the norm for all trialkylamines. There is a steric limit, however: $(i\text{-Pr})_2$NEt (Hünig's base) fails to solubilize NaHMDS in hexane, consistent with weak (transitory) solvation of LiHMDS.[14]

Solvents of intermediate donicity[47] include THF, pyridine, pyrrolidine, 1,4-dioxane, and 1,3-dioxolane (eq 7). They are characterized by forming dimers at low solvent concentrations suggested by titrations and computations to be disolvates. Exchanges of free and dimer-bound solvents are fast at −120

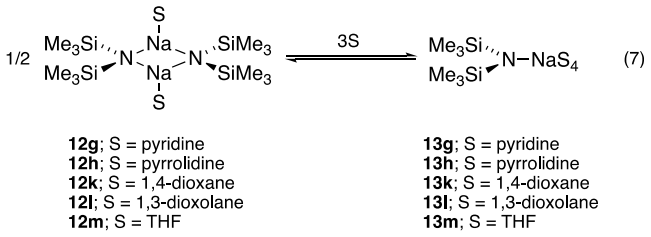

(7)

°C and at low (<1.0 equiv) levels, wherein associative substitutions would be suppressed. Even moderately elevated solvent concentrations (>0.6 M) afford monomers for THF, pyridine, and pyrrolidine. NaHMDS in THF (Table 1, entry l) is arguably the most important structural assignment based on usage,[4] prompting some comments and comparisons (Figure 11). THF-solvated dimer **12m** is isostructural to the disolvated

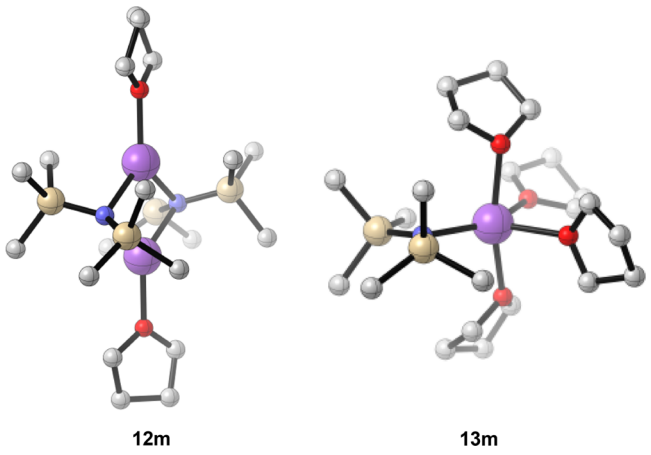

Figure 11. THF-solvated dimer **12m** and monomer **13m**.

LiHMDS and LDA dimers.[14,16] The THF-solvated NaDA dimer, by contrast, is tetrasolvated.[3] THF-solvated monomer **13m** is the sole observable form at >5 equiv of THF per sodium at −120 °C. Tetrasolvation is supported both experimentally (Figure 6) and computationally. A mixture of tri- and tetrasolvated monomers were implicated for the LiHMDS monomer.[14]

Although dioxane is technically a difunctional ligand, weak binding and the reluctance to form monomers even in neat dioxane (Figure 7) indicate it is serving as a monofunctional ligand with a lower penchant than THF to deaggregate NaHMDS. We hasten to add that the approximately 6 kcal/mol of torsional strain in the boat form of dioxane[50] accounts for why the chelated form appears to be without precedent. We witnessed gelling at low dioxane concentration even in MTBE, presumably due to linking NaHMDS dimer subunits into networks as found in monomer **9** (Chart 1).[6h]

Pyridine is shown both spectroscopically and computationally to be moderately superior to THF as a ligand for LiHMDS and other lithium salts.[14] It may find niche applications in the chemistry of NaHMDS, but a potentially greater motivation would be to understand pyridine−sodium interactions in putative[51] S_NAr reactions and other organosodium reactions of pyridine-based heterocycles.[52] Both titrations and computations suggest the dimer is disolvated. Deaggregation by pyridine is detectably more pronounced than when using THF and is computationally suggested to be a tetrasolvated monomer. Lastly, although pyridine serves as a useful chemical

https://dx.doi.org/10.1021/acs.joc.0c02546
J. Org. Chem. 2021, 86, 2406−2422

shift reagent for ^{6}Li NMR spectroscopy, we observe no notable ^{13}C, ^{15}N, or ^{29}Si shifts in [^{15}N]NaHMDS.

Pyrrolidine is representative of protic dialkylamines and is isostructural to THF. It is generally considered to be much more strongly Lewis basic than THF[53] and tetrahedral at nitrogen akin to the oxygen of THF bound to sodium.[54] Oddly, THF and pyrrolidine were indistinguishable as ligands for LiHMDS dimer, although pyrrolidine promoted deaggregation. Titration of NaHMDS with pyrrolidine (Table 1, entry h) shows a measurably more pronounced deaggregation for pyrrolidine when compared with THF, favoring a tetrasolvated monomer.

Monoalkylamines have the trappings of unhindered, highly Lewis basic solvents playing important roles in Birch reductions, S_NAr reactions of halogenated arenes and heteroarenes, ester aminolyzes, and *trans*-amidations. The monoalkylamines unencumbered by additional alkyl groups are exemplified by *n*-BuNH$_2$. Unfortunately, even at low concentrations of amine (<2.0 equiv per Na) in MTBE a coalescence is observed using ^{29}Si NMR spectroscopy, most likely due to rapid exchange of multiple species.

The attenuated basicity of NaHMDS allows us to investigate strongly coordinating dipolar solvents that would otherwise be ravaged by NaDA and other organosodiums. Hexamethylphosphoramide (HMPA) offered the best view. Titration of NaHMDS in MTBE with HMPA shows serial formation of mixed and disolvated dimers, a monomer, and an ion pair monomer (Figure 5). At ≥1.0 equiv of HMPA monomer, **13n** displays an HMPA-concentration-dependent chemical shift up to 3.0 equiv, at which point no further changes are noted. The stoichiometry and computations suggest that trisolvated monomer **13n** (n = 3) is the limiting structure. A high amount (>15 equiv) of HMPA and elevated temperature (40 °C) afford a new species, manifesting an unusually large 16.4 Hz ^{15}N−^{29}Si coupling that we attribute to ion pair **14n**. This is the only well-resolved ^{29}Si doublet for such an ion pair.

^{31}P NMR spectroscopy showed a single time-averaged resonance for the mono- and disolvated dimers and various solvated monomers. Broadening occurs at 1.0−2.0 equiv/Na, which decoalesces at 5.0 equiv of HMPA to show free HMPA and two mounds in an approximate >10:1 ratio. Monomer **13n** and ion pair **14n** are logical candidates.

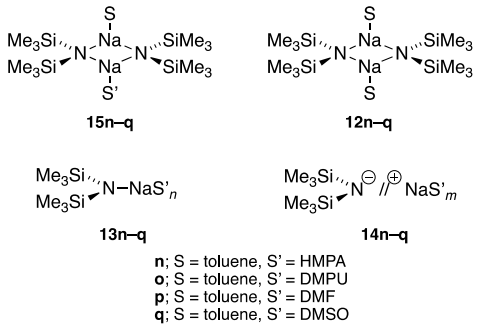

Analogous titrations of NaHMDS in MTBE with DMPU serially solvate through **15o** and **12o**. Higher DMPU concentrations cause the ^{29}Si resonance to disappear; we suspect the formation of ion pair **14o**.

Looking for dipolar solvents without the stigma of HMPA, we turned toward DMSO and DMF. Titration of NaHMDS in DMEA with DMSO at −80 °C resulted in a single ^{29}Si resonance with a DMSO-concentration-dependent chemical shift and coupling constant signifying a change from dimer to monomer. Even at low DMSO concentration, the monomer was the dominant species. However, at >3.0 equiv, a coalescence was observed. DMF performed poorly, resulting in only dimer and low concentrations of monomer at >2.0 equiv with evidence of decomposition.

Difunctional Solvents. Difunctional ligands were not as predictable as expected. The low steric demands of DME (compared with TMEDA),[14] for example, seemed likely to support doubly chelated dimer, and indeed, computations show strong binding and only limited correlated solvation. Titration of NaHMDS in DMEA with DME (Table 1, entry u) at −120 °C, however, showed a DME-solvated monomer and DMEA-solvated dimer **12d** *concurrently* at <2.0 equiv of DME, evident from an unchanged dimer coupling constant consistent with **12d**. We suspect cooperative solvation is at play here, giving rise to a DMEA−DME heterosolvated monomer at these low DME concentrations. Monomer **13v** is the sole observable form at ≥3.0 equiv. TMEDA is the quintessential bifunctional ligand that has been instrumental in shaping the thinking of researchers for generations about structure−reactivity relationships for alkali metal chemistry (eq 8).[55]

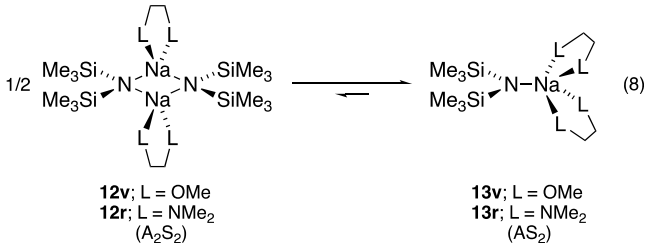

(8)

NaHMDS−TMEDA in DMEA shows a mixed-solvated dimer at <1.0 equiv and a hard end point at 1.0 equiv per sodium, which, in conjunction with MCV and ^{15}N−^{29}Si coupling data, is consistent with chelated dimer **12r** (Chart 2). Two equiv of TMEDA affords equal proportions of free and bound TMEDA in the slow exchange limit (≤−120 °C). Decoalescence of the methylene resonances in the TMEDA backbone (but not the methyls) evidences a half-chair conformer[56] exchange. Computed weakening of the second TMEDA ligand (highly correlated solvation) is affiliated with one of the four TMEDA−sodium contacts being elongated (Figure 11). This may be merely a computational overestimation of steric effects, which we have witnessed on many occasions.[57] Addition of >0.80 M (>5.0 equiv) of TMEDA forms a monomer. Five-coordinate κ^2,κ^2-**13r** is computationally viable, but four-coordinate κ^1,κ^2-**13r** is 2.0 kcal/mol more stable (Figure 12).

Analysis of the time-averaged coupling constants for both DME and TMEDA at −20 °C (Figure 13) reveals a stark contrast in the solvation energies for these two ligands. While DME forms **12v** at low concentrations (<0.50 M), TMEDA struggles to form monomer even in neat TMEDA. Overall, these results contrast with LiHMDS/DME, showing κ^1-solvated dimers and chelated monomers,[14] LDA showing only κ^1-solvated dimers,[16] and NaDA showing only κ^2-solvated dimers.[3]

(*R*,*R*)-Tetramethylcyclohexanediamine (TMCDA) often serves as a strongly coordinating TMEDA surrogate in organolithium chemistry[14,16] and has attracted some interest owing to its chirality.[58] However, the same cannot be said about NaHMDS. A single new species displaying two (diastereotopic) ^{29}Si resonances (1:1) with dimer-like coupling

https://dx.doi.org/10.1021/acs.joc.0c02546
J. Org. Chem. 2021, 86, 2406−2422

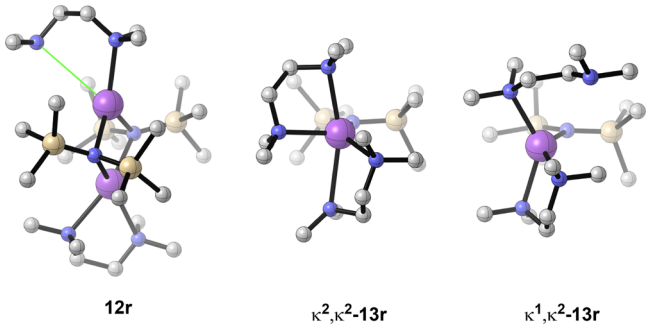

Figure 12. DFT-computed structures of TMEDA-solvated dimer **12r** showing an elongated N−Na contact and bischelated monomer **13r**.

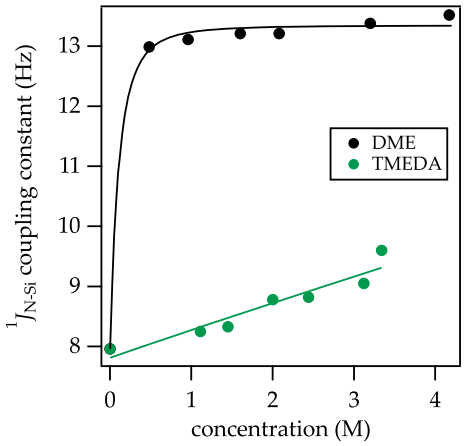

Figure 13. $^{15}N-^{29}Si$ coupling constants plotted versus [DME] (black) and [TMEDA] (green) in 2:1 pentane/toluene as cosolvent at −20 °C. The functions are fit to a model based on an $A_2S_2-AS_2$ equilibria.

persists at >3.0 equiv of TMCDA. Analogous spectroscopic data showing two distinct silyl moieties prompted O'Hara and co-workers[6d] to suggest crystallographically characterized **4** retains its structure in solution. Given the two distinct ^{29}Si resonances and the excess of DMEA, mixed-solvated analogue **15s** seems logical; however, a highly fluctional mixed-solvated open dimer of general structure **24s** cannot be excluded. To ascertain whether TMCDA fails to bind owing to unforeseen steric effects such as rigidity or poor bite angle on the larger sodium ion,[59] we compared TMEDA versus TMCDA for LiHMDS and NaHMDS monomer fragments (eq 9). Though

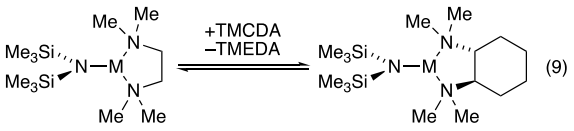

M = Li: ΔG° = −6.8 kcal/mol
M = Na: ΔG° = −5.7 kcal/mol

both LiHMDS and NaHMDS prefer TMCDA-solvated monomer over TMEDA-solvated monomer, the relative binding energy comparing lithium and sodium qualitatively suggests an elevated monomer preference for lithium.

Sparteine (**25**) has been a workhorse chiral ligand in organolithium chemistry[60] and has shown demonstrably strong binding to the LiHMDS monomer.[14] By contrast, >3.0 equiv of sparteine shows no evidence of binding to NaHMDS in DMEA (Table 1, entry s). We suspect sparteine is too sterically

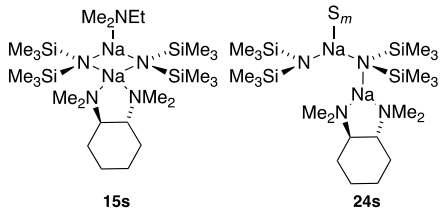

demanding to chelate to dimers or doubly chelate monomers despite crystallographic evidence that less congested sodium salts can support two bound sparteines.[61]

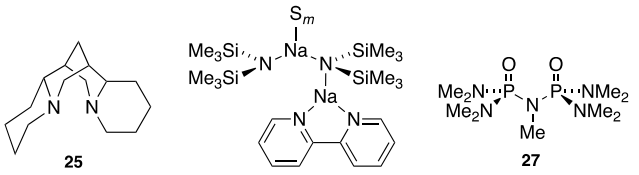

The relatively low reactivity of NaHMDS has allowed us to probe the common transition metal ligand, 2,2′-bipyridine (bipy). At 0.50 equiv of bipy in DMEA, mono- and dichelated dimers are observed. We also detect what appears to be low concentrations of open dimer (**26u**). At 1.0 to >3.0 equiv of bipy, a disolvated dimer persists to the exclusion of monomers. No spectroscopic evidence of destruction is observed after days at room temperature even though the solution color turns hot pink.

Protic amines often presented problems in studies of LiHMDS owing to facile exchanges, causing loss of $^6Li-^{15}N$ coupling. We wondered if we would have anticipated the merits of $^{15}N-^{29}Si$ coupling if the story had been different. Titrations of NaHMDS with ethylene diamine led to chronic solubility problems even using THF as the cosolvent, possibly due to intervening formation of ion pair **14** or extended hydrogen-bonded networks.[62]

N,N,N′,N″,N″-Nonamethylimidodiphosphoramide (NIPA, **27**)[63] is highly dipolar, potentially chelating, and possibly an HMPA surrogate, albeit with unknown toxicity. Unpublished work showed that NIPA affords exclusively monomeric LiHMDS.[64] NIPA has been evaluated as a ligand for a number of inorganic metal salts[65] but has been almost totally overlooked by the alkali metal community.[66,67] Although the preference of five- versus six-membered ring chelates for lithium is fully established,[14] the preference for sodium is less obvious, largely from a lack of detailed, systematic studies.[68] Unfortunately, titrations of NaHMDS with NIPA resulted in a mixture of species at ≤1.0 equiv and precipitation above 1.0 equiv: NIPA may find niches in time.

Trifunctional Solvents. We have ongoing studies of PMDTA on other sodium salts and believe it will be a ligand of central importance to the further development of organosodium chemistry; crystallographers have already discovered its merits.[1d,10] Titrations show exclusively NaHMDS monomer (eq 10) with free and bound PMDTA in slow exchange in pentane/toluene at −100 °C. NaHMDS-bound PMDTA displays seven resonances of equal intensity and two resonances corresponding to the two sets of time-averaged terminal methyl groups. Although κ^2-PMDTA-solvated dimer **12w** could afford eight carbons, MCV and large $^{15}N-^{29}Si$ coupling confirm the monomer assignment. The magnetic inequivalency of the PMDTA methylenes at low temperature and coalescence to give seven resonances of the bound form at

https://dx.doi.org/10.1021/acs.joc.0c02546
J. Org. Chem. 2021, 86, 2406−2422

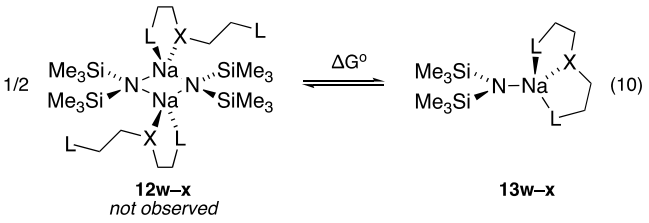

w; L = NMe_2, X = NMe; ΔG° = –7.0 kcal/mol
x; L = OMe, X = O; ΔG° = –4.7 kcal/mol

elevated temperature is consistent with half-chair conformers observed for lithium complexes of PMDTA.[14,69] DFT computations support the high preference for monomer **13w** relative to doubly chelated dimer **12w** and showed three distinct monomer conformers, of which the conformer in Figure 14 is preferred.

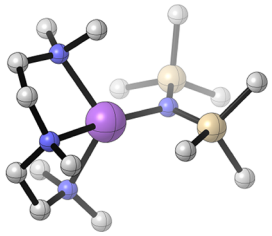

13w

Figure 14. DFT-computed lowest-energy conformer of PMDTA-complexed monomer **13w**.

Diglyme is labile to strong bases but not to NaHMDS, and it is extremely cost-effective for applications in synthesis. NaHMDS with ≥1.0 equiv of diglyme shows exclusively monomer **13x** (eq 10) with free and bound diglyme time averaged at −120 °C. Phase separation or peak broadening emblematic of ion pair formation was *not* observed. Diethylenetriamine, an unhindered analogue of PMDTA and an isostructural analogue of diglyme, by contrast afforded intractable amorphous solid even in THF solution, possibly owing to ion pair formation (see above) or hydrogen-bonded networks.[62]

Polyfunctional Solvents. In 1996, we reported that LiHMDS monomer solvated by the three parent crowns—12-crown-4 (**28**), 15-crown-5 (**29**), and 18-crown-6 (**30**)—showed two odd features that conflicted with consensus: (1) the three crowns display nearly the same binding constant (±0.5 kcal/mol) and (2) all three proved comparable to THF or TMEDA.[14] It was in this context that we investigated the binding of **28**–**30** to NaHMDS (Scheme 2).

Adding the crown ethers to NaHMDS in DMEA caused phase separation of amorphous liquids or solids. On the positive side, 15-crown-5 afforded diffractable crystals of **13z**, the first crystallographically characterized NaHMDS–crown complex (Figure 15). However, due to poor crystal quality, only atom connectivity was ascertained.

Monomer **13z** shows four Na–O close contacts (2.44–2.59 Å) that mimic two DME ligands and an elongated (2.60 Å) fifth Na–O interaction. DFT computations show similar structural features.

Titrating NaHMDS with crown ethers **28**–**30** in THF at −105 °C afforded homogeneous solutions with strong evidence of crowns remaining complexed. Titrations using

Scheme 2. Crown Ether Complexes of NaHMDS

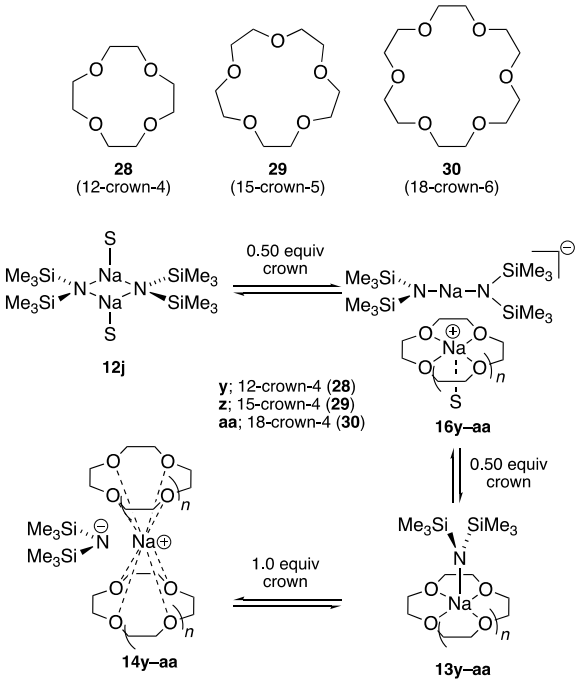

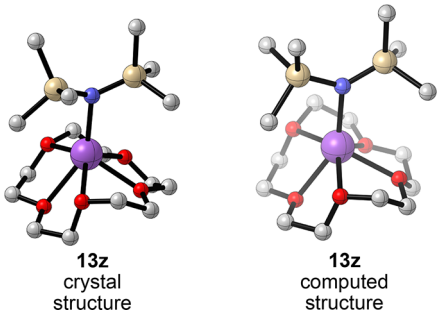

Figure 15. Crystal and computed structure of NaHMDS–15-crown-5 complex **13z**. Arrows indicate the longest Na–O contact.

NaHMDS in MTBE with 12-crown-4 converts MTBE-solvated dimer **12j** to crown-complexed monomer **13y** (1:1 stoichiometry) with no detectable intermediates. At approximately 1.5 equiv of 12-crown-4, a solid precipitates, consistent with ion pair **14y**. By contrast, 0.50 equiv of 18-crown-6 consumes >95% of MTBE-solvated dimer **12j**, affording a new species to the exclusion of other forms suggested by stoichiometry to be triple ion **16aa**. At 1.0 equiv, **16aa** is converted to exclusively monomer **13z**. Excess crown affords broad upfield ^{29}Si resonances ascribed to ion pair **14aa**. Titration with 15-crown-5 affords intermediate behavior. Triple ion **16z** and monomer **13z** are formed concurrently, with monomer **13z** becoming the sole species at 1.0 equiv. At ≥1.0 equiv of 15-crown-5, monomer **13z** crystallizes from solution. Crystallization is accelerated by warming also. Ion pair **14z** might be viable but is precluded by the crystallization.

Free and NaHMDS-monomer-bound crowns are observed in slow exchange, revealing 1:1 NaHMDS:crown stoichiometries for **29** and **30** and magnetically equivalent carbons despite computations showing significant distortions (Figure 16). High fluctionality is likely the source of the apparent high symmetry.

The evidence of triple ions **16z** and **16aa** initially was based on the substoichiometric quantities of crown required to

https://dx.doi.org/10.1021/acs.joc.0c02546
J. Org. Chem. 2021, 86, 2406–2422

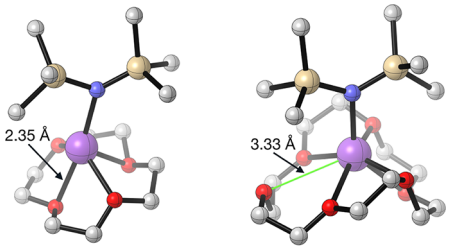

Figure 16. DFT-computed structures of crown-solvated monomers **13y** and **13aa**. Arrows designate typical Na−O bond lengths in **13y** and the longest Na−O (unbound) contact in **13aa**.

consume MTBE-solvated dimer **12j**. To confirm the assignments, a 1:1 mixture of [^{15}N]NaHMDS/NaTMDS in MTBE showing statistical mixtures of homo- and heterodimers (eq 1) was titrated with 18-crown-6, affording an ensemble of homo- and heteroaggregated triple ions (**16aa** and **30aa**). Monomers **13z** and **13aa** were also confirmed by the absence of heteroassociation. The uniquely high preference for a triple ion with 18-crown-6 may be because only 18-crown-6 can fully encapsulate the sodium within the crown (Figure 17),[70] which also impacts the binding of the MTBE cosolvent.

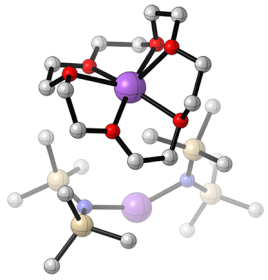

Figure 17. Computed structure of 18-crown-6-complexed triple ion **16aa**.

The final step was to compete the crowns against each other to ascertain relative affinities for NaHMDS. Titrations of NaHMDS in MTBE with stock solutions containing 1:1 mixtures of two crowns by monitoring the resolved ^{29}Si resonances revealed *nearly indistinguishable binding of the three crowns to monomer* ***13*** (Scheme 3).[71]

Polyether **31**, referred to as TDA-1, has its roots in phase transfer catalysis.[72] It displays cryptand-like behavior with LiHMDS.[14] Serial titrations of NaHMDS afford a triple ion at

Scheme 3. Competition of Crowns Showing Nearly Equal Binding to Form Monomers 13y, 13z, and 13aa

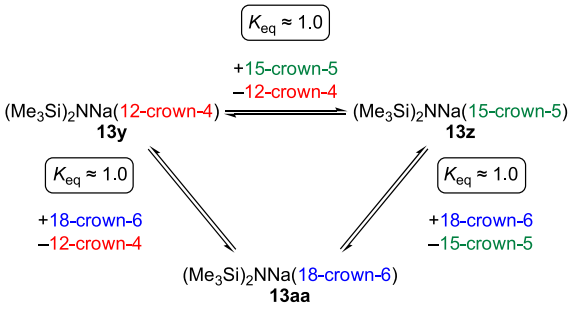

0.50 equiv that was confirmed to show a heteroassociated form when mixed with NaTMDS. Monomer **13bb** forms to the exclusion of ion pair **14bb** at ≥1.0 equiv.

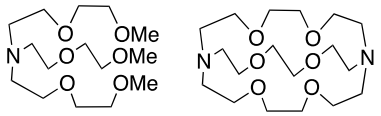

NaHMDS and cryptand [2.2.2] (**32**) in DMEA afford a white crystalline solid. An X-ray crystal structure shows the anticipated cryptate shown in Figure 18. An analogous

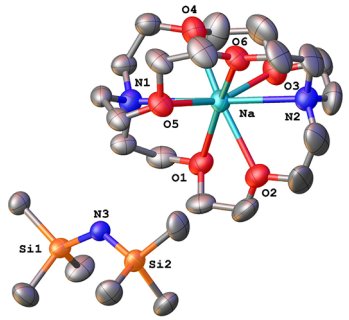

Figure 18. ORTEP drawing of **14cc** formed from NaHMDS and cryptand **32** showing thermal ellipsoids at the 50% probability level.

structure has been reported by Stephan et al. for the KHMDS·cryptand complex.[73] Addition of 0.50 equiv of **32** to NaHMDS in THF causes the disappearance of monomer **13m** and the appearance of triple-ion-based cryptate **16cc**, along with low concentrations of ion pair **14cc** as a broad mound.

Relative Solvation Capacities and Cooperative Solvation. We have described much of what we learned about the capacity of various solvents to compete with each other. We are careful not to call it solvation energy *per se* because we are comparing different structural forms. With that said, the overall capacities of solvents to *compete* are summarized in Scheme 4,

Scheme 4. Scale of Relative Competitive Binding to NaHMDS

toluene ≈ Et_3N < MTBE < TMEDA < THF < PMDTA ≈ diglyme < DME < crowns < dipolars < cryptand

using the most important solvents within their respective classes. The weakly bound ethers and trialkylamines reluctantly substitute toluene on the NaHMDS dimer but are easily displaced by ligands designated as having intermediate donicity such as THF. All but the weakest ligands also readily afford monomers at elevated ligand concentrations. A study of diamines showed TMEDA to be far superior to TMCDA. Binding of the crown ethers to the NaHMDS monomer is shockingly independent of crown structure; this result was foreshadowed by studies of LiHMDS.[14] There remained, however, a few questions central to our understanding that required explicit competitions not described above. In this context, PMDTA is a pivotal divide between moderately and strongly binding ligands and a useful benchmark.

https://dx.doi.org/10.1021/acs.joc.0c02546
J. Org. Chem. 2021, 86, 2406−2422

Competitions show that TMEDA cannot compete with THF, which was also documented for LiHMDS,[14] and THF cannot compete with PMDTA for monomer solvation. THF and other monodentate donor solvents do, however, catalyze the exchange of free and bound PMDTA as evidenced by coalescence of the PMDTA resonances in the ^{13}C NMR spectra.

Di-, tri-, and polyfunctional ethereal ligands versus PMDTA allow for the assignment of their relative binding affinities. Competing PMDTA and diglyme afford a time-averaged ^{29}Si signal, but the intermediate chemical shift suggests that **13w** and **13x** coexist. The most important comparison was, in our opinion, PMDTA and the crown ethers. In titration of NaHMDS with 1:1 stock solutions of PMDTA and 12-crown-4, the crown-solvated monomer is favored, suggesting that κ^4-polydentate ether-based monomers are favored over the κ^3-PMDTA-based monomer.[71] Furthermore, competing PMDTA and DME showed a strong preference for DME-solvated monomer **13v**. However, using this same titration method with DME and crown **28** resulted in only crown complex **13y** at 1.0 equiv of each ligand. Continued addition of both ligands resulted in an increase of the $^{15}N-^{29}Si$ coupling constant and a decrease in signal intensity, indicating cooperative solvation of an ion pair.

One might surmise that the dipolar ligands bind more strongly than PMDTA and THF. Competitions of PMDTA and HMPA show HMPA solvate **13n** to be the sole observable species. Curiously, equimolar PMDTA and HMPA at *1.0 equiv of total ligand concentration* showed a new ^{29}Si signal corresponding to low concentrations of triple ion, suggesting cooperative solvation is at play. It reminds us that combinations of *two* ligands may *cooperatively* provide access to atypical aggregation states.

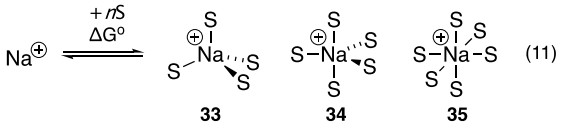

33 34 35

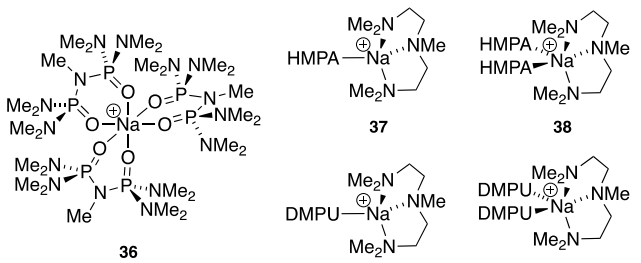

36 37 38 39 40

Sodium Cation Solvation. The solvation energies of sodium cations were calculated (Table 2), filling what appears to be a gap in the computational literature. These computed energies could guide synthetic chemists hoping to markedly enhance reactivity via ionization and to the sodium battery community.[74−76] The relative energies corroborate the experimentally determined solvent hierarchy. For example, confirmed ion-pair-forming ligands such as cryptand **32** and HMPA show greater solvation energies than THF, which does not ionize NaHMDS. Furthermore, the solvation energy of the PMDTA-mixed solvates **37**−**40** demonstrates plausibility for cooperative solvation.

Table 2. Solvation Energies of Sodium Cations

ligand	cation	$\Delta G°$ (kcal/mol)
THF	**33m**	−66.5
	34m	−71.7
	35m	−78.5
HMPA	**33n**	−100.2
DMPU	**33o**	−92.8
DMF	**34p**	−103.3
DMSO	**34q**	−97.5
DME	**35v**	−80.0
PMDTA	**35w**	−77.4
diglyme	**35x**	−82.2
12-crown-4	$^{+}Na(crown)_2$	−88.2
15-crown-5	$^{+}Na(crown)_2$	−91.5
18-crown-6	$^{+}Na(crown)_2$	−76.6
TDA-1	$^{+}Na(TDA)$	−90.0
C222	$^{+}Na(crypt)$	−103.7
NIPA	**36**	−115.7
PMDTA + *n*HMPA	**37**	−81.4
	38	−96.4
PMDTA + *n*DMPU	**39**	−80.0
	40	−92.4

CONCLUSION

Exploration of NaHMDS dissolved in >30 solvents showed a dominance of disolvated dimers in neat, weakly coordinating solvents and at low concentrations of strongly coordinating monodentate solvents. Intermediate and strongly coordinating solvents as well as a bevy of di-, tri-, and polyfunctional solvents (usually called ligands) elicited deaggregation without exception. Experimental evidence in conjunction with extensive DFT computations implicated monomers with four- and five-coordinate sodium to be the norm. Ionizations in dipolar and polydentate ligands in the form of both triple ions and ion pairs offer interesting views of sodium cation solvation. On several occasions open dimers were detected, although the evidence was not unassailable.

Most solvents behaved as one might expect when placed in the context of LDA, LiHMDS, and NaDA, but not always. TMCDA and sparteine are relatively good ligands for LiHMDS and other organolithiums but show low affinities for NaHMDS. We are reminded of the ultimate truism: sodium and lithium are different metals. Three crown ethers—12-crown-4, 15-crown-5, and 18-crown-6—showed high affinities for NaHMDS but defy consensus by displaying nearly identical binding constants. We suspect few would have predicted this. Probes of relative affinities using binary mixtures uncovered several examples of cooperative solvation, offering creative opportunities to control structure while reminding us that solvent mixtures bring complexities that must be respected. Moreover, substrate complexation during a reaction is merely a variant of cooperative solvation.

Often new tactical advances emerge from a study that expand our toolkit. The standout example in this study was showing that $^{15}N-^{29}Si$ coupling first studied by Lukevics and co-workers correlates strongly with the NaHMDS aggregation state. ^{29}Si NMR spectroscopy offered a stupendously convenient window into structure in a variety of solvents over a range of temperatures. We must confess that during studies of [^{6}Li,^{15}N]LiHMDS we never recorded ^{29}Si NMR spectra.[14] (We did not need them.) Belatedly, we find that correlations of $^{15}N-^{29}Si$ hold up, albeit with some quantitative

https://dx.doi.org/10.1021/acs.joc.0c02546
J. Org. Chem. 2021, 86, 2406−2422

differences when compared to NaHMDS (see **41** and **42**). We imagine broader applications to M−N(SiR_3)$_2$. Moreover, the ease of recording high-quality ^{29}Si NMR spectra suggests tremendous promise akin to tagging a reagent with ^{19}F.[77] Casual survey of the literature suggests that, despite the prevalence of silyl groups and silyl-based protecting groups, ^{29}Si NMR spectroscopy is being underutilized.[78] It would be a superb tool to monitor reactions and products by the organic synthesis community. We also optimized the basis set, functionals, and grid size for DFT computations of sodium salts to improve our previous protocols. The computations proved invaluable, but the correlations of theory and experiment are qualitative.

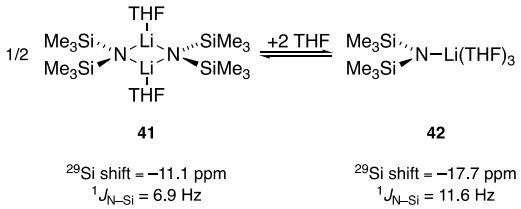

What is gained by knowing detailed structures of NaHMDS beyond merely plugging a glaring hole in the organosodium literature? The empirically minded consumers now have a large choice of solvents and can, at least in principle, pursue changes in reactivity and selectivity by targeting observable changes in the underlying aggregation and solvation states. Of course, the mechanism is more complex than that, but it is a start. We hasten to add that it would be difficult to predict something as simple as the solvent-dependent relative reactivities of NaHMDS. Do they span an order of magnitude or 6 orders of magnitude? We also have a particular fondness for affiliating solvent-dependent rates and selectivities with explicit changes in the mechanisms. The assigned solvation and aggregation states of NaHMDS are non-negotiable prerequisites to ongoing detailed mechanistic studies.

The potential synthetic importance of several of the solvents is worthy of comment. MTBE cleanly affords exclusively disolvated dimer and seems like it may be the cosolvent of choice when additional ligands are added. Similarly, some stellar properties of LiHMDS/Et_3N/toluene[15] in conjunction with foreshadowing from NaHMDS/Et_3N-mediated enolizations of acylated oxazolidinones to generate Evans enolates[15] suggest NaHMDS/Et_3N/toluene could offer superior reactivities at low cost. Ongoing studies of NaDA suggest that PMDTA may play a central role in organosodium chemistry. Lastly, although NaTMDS only supported MCV studies, we wonder if NaTMDS may have undiscovered reactivities, especially for C−N bond-forming nucleophilic reactions demanding a smaller nucleophile.

EXPERIMENTAL SECTION

Reagents and Solvents. Hydrocarbons, monofunctional trialkylamines, monofunctional ethers, HMPA, TMEDA, (*R*,*R*)-TMCDA, (−)-sparteine, PMDTA, and diglyme were distilled from blue or purple solutions containing sodium benzophenone ketyl. Styrene, DMPU, DMF, DMSO, 12-crown-4, 15-crown-5, and TDA-1 were dried over 4 Å mol sieves prior to use. Bipyridine and [2.2.2]-cryptand were purchased and used without purification. 18-crown-6 was distilled.

NMR Spectroscopic Analyses. An NMR tube under vacuum was flame-dried on a Schlenk line, allowed to cool to room temperature, backfilled with argon, placed in a −78 °C dry ice/acetone bath, and charged with NaHMDS and solvents using stock solutions. The sample was mixed with a vortex mixer. Standard ^{1}H, ^{13}C, ^{15}N, and ^{29}Si spectra were recorded on a 500 MHz spectrometer at 500, 125.79, 50.66, and 99.36 MHz, respectively. The chemical shifts are referenced at −120 °C as follows: ^{1}H (Me_4Si, 0.0 ppm), ^{13}C (Me_4Si, 0.0 ppm), ^{15}N (neat Me_2NEt, 25.7 ppm), and ^{29}Si (Me_4Si, 0.0 ppm).

[^{15}N]Hexamethyldisilazane. [^{15}N]NH_3 was generated by a known procedure[12] by mixing [^{15}N]ammonium chloride (3.0 g, 55.0 mmol, >99% ^{15}N isotopic purity) with 6.00 g (150 mmol) of granular NaOH in a 25 mL one-neck round-bottom flask equipped with an NaOH-filled tube through which the ammonia gas is transferred to an empty 100 mL round-bottom flask cooled to −78 °C (see Supporting Information). The mixture was warmed with a heat gun for approximately 20 min. After the transfer of ammonia was complete, 1-(trimethylsilyl)imidazole (14.7 g, 15.3 mL, 105 mmol, 98% purity) was added at −78 °C with stirring. Imidazole precipitated immediately, after which anhydrous diethyl ether (20 mL) was added to the flask, and the mixture was held at 0 °C for 40 min. Cholesterol (3.0 g) was added to the [^{15}N]hexamethyldisilazane with stirring for 45 min to remove excess 1-(trimethylsilyl)imidazole. Short path distillation at atmospheric pressure removed the diethyl ether. Vacuum distillation (40 mmHg, 20 °C) afforded 4.75 mL (47% yield) of (Me_3Si)$_2$^{15}NH.

[^{15}N]-Sodium Hexamethyldisilazide (1). [^{15}N]NaHMDS was prepared following a known procedure.[12] To a flame-dried fine-mesh swivel-frit setup was added sliced sodium metal (1.20 g, 52.4 mmol) in a glovebox. The apparatus was moved to a Schlenk line for the remainder of the procedure. Under argon, [^{15}N]HMDS (7.31 g, 9.45 mL, 45.0 mmol) and 40 mL of DMEA were added to the reaction flask at room temperature. Isoprene (2.62 mL, 26.2 mmol) dissolved in 8 mL of dry DMEA was then added over 1 h via syringe pump to the mixture. After addition of isoprene, the reaction was stirred at RT for an additional 2 h. The solution was subsequently filtered through a frit, transferred with a canula to a second swivel coarse-frit setup, and vacuum evaporated to dryness for at least 10 h to yield a white powder. The powder was suspended in dry pentane (∼20 mL), stirred for 1 h, and filtered. Finally, the product was washed with 20 mL of pentane and yielded 6.70 g (91% yield) of [^{15}N]NaHMDS as a white solid,[12] which was transferred to a glovebox and stored at room temperature. NaHMDS can be recrystallized as previously described[12] but with no detectable improvement. ^{1}H NMR (toluene-d_8, 500 MHz): δ 0.2 (s, 18 H). ^{13}C{^{1}H} NMR (toluene-d_8, 125.72 MHz): δ 6.8 (d, $^2J_{N-C}$ = 2.7 Hz). ^{29}Si NMR (toluene-d_8, 99.36 MHz): δ −14.4 (d, $^1J_{N-Si}$ = 7.9 Hz).

Sodium Tetramethyldisilazide (NaTMDS, 17). NaTMDS was synthesized from 1,1,3,3-tetramethyldisilazane using the prep described for NaHMDS, affording NaTMDS (**17**) as a white solid (3.0 g, 50% yield).[17] ^{13}C{^{1}H} NMR (toluene-d_8, 125.72 MHz): δ 5.9. ^{29}Si NMR (toluene-d_8, 99.36 MHz): δ −25.7.

Sodium Bis(dimethyl(phenyl)silyl)amide (NaDPTMDS, 18). NaDPTMDS was synthesized from bis(dimethyl(phenyl)silyl)amine using the same prep described for NaHMDS, affording NaDPTMDS (**18**) as a white solid (5.3 g, 45% yield).[18] ^{13}C{^{1}H} NMR (125.72 MHz, toluene-d_8): δ 148.6, 133.2, 5.5.

Sodium 1-Aza-2,2,5,5-tetramethyl-2,5-disilacyclopentane (19). Sodiated 1-aza-2,2,5,5-tetramethyl-2,5-disilacyclopentane was prepared using the same dissolving-metal-based prep described previously for NaHMDS, affording **19** as a white solid (3.4 g, 70% yield).[19] ^{13}C{^{1}H} NMR (125.72 MHz, DMEA): δ 13.2, 6.3.

Crystallization Conditions (13z and 14cc). To a flame-dried NMR tube under Ar was added 600 μL of 0.10 M NaHMDS in DMEA at room temperature. Next, 1.0 equiv of ligand was added to the tube, which immediately resulted in a crystallization event. The tube was then sealed under partial vacuum. Recrystallization of each complex was conducted by simply running crystals suspended in DMEA under hot tap water followed by slow cooling until they reached room temperature.

https://dx.doi.org/10.1021/acs.joc.0c02546
J. Org. Chem. 2021, 86, 2406−2422

■ ASSOCIATED CONTENT

Supporting Information

The Supporting Information is available free of charge at https://pubs.acs.org/doi/10.1021/acs.joc.0c02546.

Spectroscopic data, rate, and computational data (PDF)

Accession Codes

CCDC 2042630 contains the supplementary crystallographic data for this paper. These data can be obtained free of charge via www.ccdc.cam.ac.uk/data_request/cif, or by emailing data_request@ccdc.cam.ac.uk, or by contacting The Cambridge Crystallographic Data Centre, 12 Union Road, Cambridge CB2 1EZ, UK; fax: +44 1223 336033.

■ AUTHOR INFORMATION

Corresponding Author

David B. Collum − *Department of Chemistry and Chemical Biology Baker Laboratory, Cornell University, Ithaca, New York 14853−1301, United States;* orcid.org/0000-0001-6065-1655; Email: dbc6@cornell.edu

Author

Ryan A. Woltornist − *Department of Chemistry and Chemical Biology Baker Laboratory, Cornell University, Ithaca, New York 14853−1301, United States*

Complete contact information is available at: https://pubs.acs.org/10.1021/acs.joc.0c02546

Notes

The authors declare no competing financial interest.

■ ACKNOWLEDGMENTS

We thank the National Institutes of Health (GM131713) for support and Samantha N. MacMillan for the crystal structures.

■ REFERENCES

(1) (a) Seyferth, D. Alkyl and Aryl Derivatives of the Alkali Metals: Useful Synthetic Reagents as Strong Bases and Potent Nucleophiles. 1. Conversion of Organic Halides to Organoalkali-Metal Compounds. *Organometallics* **2006**, *25*, 2. (b) Seyferth, D. Alkyl and Aryl Derivatives of the Alkali Metals: Strong Bases and Reactive Nucleophiles. 2. Wilhelm Schlenk's Organoalkali-Metal Chemistry. The Metal Displacement and the Transmetalation Reactions. Metalation of Weakly Acidic Hydrocarbons. Superbases. *Organometallics* **2009**, *28*, 2. (c) Lochmann, L.; Janata, M. 50 Years of Superbases Made from Organolithium Compounds and Heavier Alkali Metal Alkoxides. *Eur. J. Chem.* **2014**, *12*, 537. (d) Robertson, S. D.; Uzelac, M.; Mulvey, R. E. Alkali-Metal-Mediated Synergistic Effects in Polar Main Group Organometallic Chemistry. *Chem. Rev.* **2019**, *119*, 8332.

(2) Woltornist, R. A.; Ma, Y.; Algera, R. F.; Zhou, Y.; Zhang, Z.; Collum, D. B. Structure, Reactivity, and Synthetic Applications of Sodium Diisopropylamide. *Synthesis* **2020**, *52*, 1478.

(3) Algera, R. F.; Ma, Y.; Collum, D. B. Sodium Diisopropylamide: Aggregation, Solvation, and Stability. *J. Am. Chem. Soc.* **2017**, *139*, 7921.

(4) Sodium hexamethyldisilazide. In *e-EROS Encyclopedia of Reagents for Organic Synthesis*; Watson, B. T.; Lebel, H., Eds.; John Wiley & Sons: New York, 2005; pp 1−10.

(5) (a) Stumpf, A.; Cheng, Z. K.; Wong, B.; Reynolds, M.; Angelaud, R.; Girotti, J.; Deese, A.; Gu, C.; Gazzard, L. Development of an Expedient Process for the Multi-Kilogram Synthesis of Chk1 Inhibitor GDC-0425. *Org. Process Res. Dev.* **2015**, *19*, 661. (b) Kerdesky, F. A. J.; Leanna, M. R.; Zhang, J.; Li, W.; Lallaman, J. E.; Ji, J.; Morton, H. E. An Efficient Multikilogram Synthesis of ABT-963: A Selective COX-2 Inhibitor. *Org. Process Res. Dev.* **2006**, *10*, 512. (c) Butters, M.; Ebbs, J.; Green, S. P.; MacRae, J.; Morland, M. C.; Murtiashaw, C. W.; Pettman, A. J. Process Development of Voriconazole: A Novel Broad-Spectrum Triazole Antifungal Agent. *Org. Process Res. Dev.* **2001**, *5*, 28. (d) Fuerstner, A.; Fenster, M. D. B.; Fasching, B.; Godbout, C. P.; Radkowski, K. Toward the Total Synthesis of Spirastrellolide A. Part 2: Conquest of the Northern Hemisphere. *Angew. Chem., Int. Ed.* **2006**, *45*, 5510. (e) Davis, F. A. Recent Applications of *N*-Sulfonyloxaziridines (Davis oxaziridines) in Organic Synthesis. *Tetrahedron* **2018**, *74*, 3198. (f) Rao, K. S.; St-Jean, F.; Kumar, A. Quantitation of a Ketone Enolization and a Vinyl Sulfonate Stereoisomer Formation Using Inline IR Spectroscopy and Modeling. *Org. Process Res. Dev.* **2019**, *23*, 945.

(6) (a) **1**: Driess, M.; Pritzkow, H.; Skipinski, M.; Winkler, U. Synthesis and Solid State Structures of Sterically Congested Sodium and Cesium Silyl(fluorosilyl)phosphanide Aggregates and Structural Characterization of the Trimeric Sodium Bis(trimethylsilyl)amide. *Organometallics* **1997**, *16*, 5108. (b) **2**: Kennedy, A. R.; Mulvey, R. E.; O'Hara, C. T.; Robertson, S. D.; Robertson, G. M. Catena-Poly[Sodium-μ_2-(*N,N,N′,N′*- Tetramethylethane-1,2-Diamine)-y^2-*N,N′*-Sodium- Bis[μ_2-Bis(Trimethylsilyl)Azanido−^{2} *N:N*]]. *Acta Crystallogr., Sect. E: Struct. Rep. Online* **2012**, *68*, No. m1468. (c) **3**, **10**, and **11**: Schuler, P.; Gorls, H.; Westerhausen, M.; Krieck, S. Bis(trimethylsilyl)amide Complexes of s-Block Metals with Bidentate Ether and Amine Ligands. *Dalton Trans.* **2019**, *48*, 8966. (d) **4** and **5**: Ojeda-Amador, A. I.; Martínez-Martínez, A. J.; Kennedy, A. R.; Armstrong, D. R.; O'Hara, C. T. Monodentate Coordination of the Normally Chelating Chiral Diamine (*R,R*)-TMCDA. *Chem. Commun.* **2017**, *53*, 324. (e) **6**: Sarazin, Y.; Coles, S. J.; Hughes, D. L.; Hursthouse, M. B.; Bochmann, M. Cationic Brønsted Acids for the Preparation of Sn(IV) Salts: Synthesis and Characterisation of $[Ph_3Sn(OEt_2)][H_2N\{B(C_6F_5)_3\}_2]$,$[Sn(NMe_2)_3(HNMe_2)_2][B(C_6F_5)_4]$ and $[Me_3Sn(HNMe_2)_2][B(C_6F_5)_4]$. *Eur. J. Inorg. Chem.* **2006**, *2006*, 3211. (f) **7**: Karl, M.; Seybert, G.; Massa, W.; Harms, K.; Agarwal, S.; Maleika, R.; Stelter, W.; Greiner, A.; Neumüller, W. H.; Dehnicke, K. Amidometallate von Seltenerdelementen. Synthese Und Kristallstrukturen von $[Na(12\text{-Krone-}4)_2][M\{N(SiMe_3)_2\}_3(OSiMe_3)]$ (M = Sm, Yb), $[Na(THF)_3Sm\{N(SiMe_3)_2\}_3(C{\equiv}C\text{-}Ph)]$, $[Na(THF)_6][Lu_2(\mu\text{-}NH_2)(\mu\text{-}NSiMe_3)\{N(SiMe_3)_2\}_4]$ Sowie von $[NaN(SiMe_3)_2(THF)]_2$. *Z. Anorg. Allg. Chem.* **1999**, *625*, 1301. (g) **8**: Neufeld, R.; Michel, R.; Herbst-Irmer, R.; Schöne, R.; Stalke, D. Introducing a Hydrogen-Bond Donor into a Weakly Nucleophilic Brønsted Base: Alkali Metal Hexamethyldisilazides (MHMDS, M = Li, Na, K, Rb, and Cs) with Ammonia. *Chem. - Eur. J.* **2016**, *22*, 12340. (h) **9**: Edelmann, F. T.; Pauer, F.; Wedler, M.; Stalke, D. Preparation and Structural Characterization of Dioxane Coordinated Alkali Metal Bis(Trimethylsilyl)Amides. *Inorg. Chem.* **1992**, *31*, 4143. (i) For a NaHMDS−sodium enolate mixed aggregate characterized crystallographically, see: Williard, P. G.; Hintze, M. J. Mixed Aggregates: Crystal Structures of a Lithium Ketone Enolate/Lithium Amide and of a Sodium Ester Enolate/Sodium Amide. *J. Am. Chem. Soc.* **1990**, *112*, 8602.

(7) (a) Knapp, C.; Lork, E.; Borrmann, T.; Stohrer, W.-D.; Mews, R. Versuche Zur Darstellung Vont-$BuCN_5S_3$ Und Die Unerwartete Isolierung Einer Kovalenten Modifikation von Tetraschwefelpentastickstoff-Chlorid S_4N_5Cl. *Z. Anorg. Allg. Chem.* **2005**, *631*, 1885. (b) Clark, N. M.; García-Álvarez, P.; Kennedy, A. R.; O'Hara, C. T.; Robertson, G. M. Reactions of (−)-Sparteine with Alkali Metal HMDS Complexes: Conventional Meets the Unconventional. *Chem. Commun.* **2009**, *39*, 5835. (c) Williard, P. G.; Nichols, M. A. Structural Characterization of Mixed Alkali Metal Bis(trimethylsilyl) Amide Bases. *J. Am. Chem. Soc.* **1991**, *113*, 9671.

(8) Ojeda-Amador, A. I.; Martinez-Martinez, A. J.; Kennedy, A. R.; O'Hara, C. T. Synthetic and Structural Studies of Mixed Sodium Bis(trimethylsilyl) Amide/Sodium Halide Aggregates in the Presence of η^2-*N,N*-, η^3-*N,N,N/N,O,N*-, and η^4-*N,N,N,N*-donor Ligands. *Inorg. Chem.* **2015**, *54*, 9833.

(9) Kupce, E.; Lukevics, E.; Varezhkin, Y. M.; Mikhailova, A. N.; Sheludyakov, V. D. Silicon-29-Nitrogen-15 Spin-Spin Coupling

Constants in Silazanes. *Organometallics* **1988**, *7*, 1649. and references cited therein.
(10) For an extensive review on the chemistry of the alkali metal amides, see: Mulvey, R. E.; Robertson, S. D. Synthetically Important Alkali-Metal Utility Amides: Lithium, Sodium, and Potassium Hexamethyldisilazides, Diisopropylamides, and Tetramethylpiperidides. *Angew. Chem., Int. Ed.* **2013**, *52*, 11470.
(11) Luo, G.; Luo, Y.; Qu, J. Direct Nucleophilic Trifluoromethylation Using Fluoroform: a Theoretical Mechanistic Investigation and Insight into the Effect of Alkali Metal Cations. *New J. Chem.* **2013**, *37*, 3274.
(12) Woltornist, R. A.; Collum, D. B. Using ^{15}N-^{29}Si Scalar Coupling to Determine Aggregation and Solvation States. *J. Am. Chem. Soc.* **2020**, *142*, 6852.
(13) Many of the results for LiHMDS and LDA can be accessed through two review articles.[14,16] More recent studies not cited therein are provided below.[15]
(14) Lucht, B. L.; Collum, D. B. Lithium Hexamethyldisilazide: A View of Lithium Ion Solvation Through a Glass-Bottom Boat. *Acc. Chem. Res.* **1999**, *32*, 1035.
(15) Snaddon, T. N.; Buchgraber, P.; Schulthoff, S.; Wirtz, C.; Mynott, R.; Fürstner, A. Total Synthesis of Berkelic Acid. *Chem. - Eur. J.* **2010**, *16*, 12133.
(16) Collum, D. B. Solution Structures of Lithium Dialkylamides and Related *N*-Lithiated Species: Results from ^{6}Li-^{15}N Double Labeling Experiments. *Acc. Chem. Res.* **1993**, *26*, 227.
(17) (a) Eppinger, J.; Herdtweck, E.; Anwander, R. Synthesis and Characterisation of Alkali Metal Bis(Dimethylsilyl) Amides: Infinite All-Planar Laddering in the Unsolvated Sodium Derivative. *Polyhedron* **1998**, *17*, 1195. (b) Schneider, J.; Popowski, E.; Reinke, H. Darstellung, Charakterisierung Und Reaktionsverhalten von Natrium- Und Kaliumhydridosilylamiden $R_2(H)Si\text{-}N(M)R'$ (M = Na, K) - Kristallstruktur von $[(ME_3C)_2(H)Si\text{-}N(K)SiMe_3]_2 \cdot$THF. *Z. Anorg. Allg. Chem.* **2003**, *629*, 55.
(18) Evans, W. J.; Rego, D. B.; Ziller, J. W. Lanthanum and Alkali Metal Coordination Chemistry of the Bis(Dimethylphenylsilyl)Amide Ligand. *Inorg. Chem.* **2006**, *45*, 3437.
(19) 1-Aza-2,2,5,5-tetramethyl-2,5-disilacyclopentane preparation: Baney, R. H.; Haberland, G. G. The Question of Flexibility Around the Silicon-Nitrogen Bond in Polysilazanes. A Comparison with Polysiloxanes. *J. Organomet. Chem.* **1966**, *5*, 320−325.
(20) Frisch, M. J.; Trucks, G. W.; Schlegel, H. B.; Scuseria, G. E.; Robb, M. A.; Cheeseman, J. R.; Zakrzewski, V. G.; Montgomery, J. A., Jr.; Stratmann, R. E.; Burant, J. C.; Dapprich, S.; Millam, J. M.; Daniels, A. D.; Kudin, K. N.; Strain, M. C.; Farkas, O.; Tomasi, J.; Barone, V.; Cossi, M.; Cammi, R.; Mennucci, B.; Pomelli, C.; Adamo, C.; Clifford, S.; Ochterski, J.; Petersson, G. A.; Ayala, P. Y.; Cui, Q.; Morokuma, K.; Malick, D. K.; Rabuck, A. D.; Raghavachari, K.; Foresman, J. B.; Cioslowski, J.; Ortiz, J. V.; Baboul, A. G.; Stefanov, B. B.; Liu, G.; Liashenko, A.; Piskorz, P.; Komaromi, I.; Gomperts, R.; Martin, R. L.; Fox, D. J.; Keith, T.; Al-Laham, M. A.; Peng, C. Y.; Gill, A.; Nanayakkara, C.; Gonzalez, M.; Challacombe, P. M. W.; Johnson, B.; Chen, W.; Wong, M. W.; Andres, J. L.; Gonzalez, C.; Head-Gordon, M.; Replogle, E. S.; Pople, J. A. *Gaussian 09*, Revision A.02; Gaussian, Inc.: Wallingford, CT, 2009.
(21) Zhao, Y.; Truhlar, D. G. The M06 Suite of Density Functionals for Main Group Thermochemistry, Thermochemical Kinetics, Noncovalent Interactions, Excited States, and Transition Elements: Two New Functionals and Systematic Testing of Four M06-Class Functionals and 12 Other Functionals. *Theor. Chem. Acc.* **2008**, *120*, 215.
(22) Several seemingly simple computations at the MP2 level of theory failed for reasons that were unclear. This is *not* a problem using DFT with M06 functionals.
(23) Weigend, F.; Ahlrichs, R. Balanced Basis Sets of Split Valence, Triple Zeta Valence and Quadruple Zeta Valence Quality for H to Rn: Design and Assessment of Accuracy. *Phys. Chem. Chem. Phys.* **2005**, *7*, 3297.
(24) Legault, C. Y. *CYLview, 1.0b*; Université de Sherbrooke, 2009 (http://www.cylview.org).
(25) Bootsma, A. N.; Wheeler, S. Popular Integration Grids Can Result in Large Errors in DFT-Computed Free Energies. *ChemRxiv* **2019**.
(26) For example, the solvation energies of toluene on NaHMDS dimer decreased by 2.0 kcal/mol by switching from a grid size of 75 302 to 99 590.
(27) Yang, Z.; Yang, S.; Yu, P.; Li, Y.; Doubleday, C.; Park, J.; Patel, A.; Jeon, B.-s.; Russell, W. K.; Liu, H.-w.; Russell, D. H.; Houk, K. N. Influence ofwater and enzyme SpnF on the dynamics and energetics of the ambimodal [6 + 4]/[4 + 2] cycloaddition. *Proc. Natl. Acad. Sci. U. S. A.* **2018**, *115*, E848.
(28) Renny, J. S.; Tomasevich, L. L.; Tallmadge, E. H.; Collum, D. B. Method of Continuous Variations: Applications of Job Plots to the Study of Molecular Associations in Organometallic Chemistry. *Angew. Chem., Int. Ed.* **2013**, *52*, 11998.
(29) The *intended* mole fraction refers to the mole fraction based on what was added to the samples. The *measured* mole fraction—the mole fraction within only the ensemble of interest—eliminates the distorting effects of impurities. This problem has been highlighted: Brynn Hibbert, D.; Thordarson, P. The Death of the Job Plot, Transparency, Open Science and Online Tools, Uncertainty Estimation Methods and Other Developments in Supramolecular Chemistry Data Analysis. *Chem. Commun.* **2016**, *52*, 12792.
(30) Job, P. Formation and Stability of Inorganic Complexes in Solution. *Ann. Chim.* **1928**, *9*, 113.
(31) The concentration of NaHMDS, although expressed in units of molarity, refers to the concentration of the monomer subunit (normality).
(32) Yamada, S. Cation-π Interactions in Organic Synthesis. *Chem. Rev.* **2018**, *118*, 11353.
(33) Neufeld, R.; John, M.; Stalke, D. The Donor-Base-Free Aggregation of Lithium Diisopropyl Amide in Hydrocarbons Revealed by a DOSY Method. *Angew. Chem., Int. Ed.* **2015**, *54*, 6994.
(34) Lambert, C.; von Ragué Schleyer, P. Are Polar Organometallic Compounds "Carbanions"? The Gegenion Effect on Structure and Energies of Alkali-Metal Compounds. *Angew. Chem., Int. Ed. Engl.* **1994**, *33*, 1129.
(35) (a) Eastham, J. F.; Gibson, G. W. Solvent Effects in Organometallic Reactions. II. *J. Am. Chem. Soc.* **1963**, *85*, 2171. (b) Bartlett, P. D.; Goebel, C. V.; Weber, W. P. Ethylenation of Secondary and Tertiary Alkyllithiums. II. Its Kinetics and the Nature of the Active Species. *J. Am. Chem. Soc.* **1969**, *91*, 7425. (c) Lewis, H. L.; Brown, T. L. Association of Alkyllithium Compounds in Hydrocarbon Media. Alkyllithium-Base Interactions. *J. Am. Chem. Soc.* **1970**, *92*, 4664. (d) Popov, A. I. Alkali Metal NMR and Vibrational Spectroscopic Studies on Solvates in Non-aqueous Solvents. *Pure Appl. Chem.* **1975**, *41*, 275.
(36) Double solvation of dimer follows a first- rather than second-order saturation function because of a single solvent per sodium.
(37) (a) Reich, H. J. Role of Organolithium Aggregates and Mixed Aggregates in Organolithium Mechanisms. *Chem. Rev.* **2013**, *113*, 7130. (b) Hilmersson, G.; Davidsson, O. A Multinuclear NMR-Study of a Chiral Lithium Amide with an Intramolecular Chelating Methoxy Group in Coordinating Solvents at the Slow Ligand-Exchange Limit. *J. Org. Chem.* **1995**, *60*, 7660. (c) Hilmersson, G.; Ahlberg, P.; Davidsson, O. Enantiomeric Perturbation of Equilibria. Differential Solvation of a Chiral Lithium Amide by the Enantiomers of 2-Methyltetrahydrofuran Measured by NMR Spectroscopy. *J. Am. Chem. Soc.* **1996**, *118*, 3539.
(38) We use the term "cooperative" for advantageous (protagonistic) influences of two coordinated solvents. The term "correlated" is intended as a neutral term in which two or more coordinated solvents influence their relative binding irrespective of whether protagonistically or antagonistically.[40] Correlated ligation is an issue across all metals.[41] There is also a statistical factor in a serial substitution that is easily overlooked.[42]

https://dx.doi.org/10.1021/acs.joc.0c02546
J. Org. Chem. 2021, 86, 2406−2422

(39) Hoffmann, D.; Collum, D. B. Competitive and Cooperative Binding of Vicinal Diamines to *n*-Butyllithium Dimers: Relationship of Ligand Structure and Relative Solvation Energies. *J. Am. Chem. Soc.* **1998**, *120*, 5810.
(40) For investigations of correlated phosphine binding on transition metals, see: Li, C.; Oliván, M.; Nolan, S.; Caulton, K. G. *Organometallics* **1997**, *16*, 4223. and references cited therein.
(41) (a) Benson, S. W. Statistical Factors in the Correlation of Rate Constants and Equilibrium Constants. *J. Am. Chem. Soc.* **1958**, *80*, 5151. (b) Fay, R. C.; Lowry, R. N. Proton Magnetic Resonance Studies of Ligand-Exchange Equilibriums for Dihalo- and Diethoxybis(*beta*-diketonato)titanium(IV) Complexes. *Inorg. Chem.* **1974**, *13*, 1309.
(42) The computations use the Gaussian standard state of 1.0 atm. If the solvent concentration is corrected to neat solvent (approximately 10 M), each solvation step benefits from approximately 2.0 kcal/mol of additional stabilization at −78 °C (195 K). Pratt, L. M.; Merry, S.; Nguyen, S. C.; Quan, P.; Thanh, B. T. A Computational Study of Halomethyllithium Carbenoid Mixed Aggregates with Lithium Halides and Lithium Methoxide. *Tetrahedron* **2006**, *62*, 10821.
(43) From Wikipedia, "an isodesmic reaction is a chemical reaction in which the type of chemical bonds broken in the reactant are the same as the type of bonds formed in the reaction product".
(44) Ojeda-Amador, A. I.; Martinez-Martinez, A. J.; Robertson, G. M.; Robertson, S. D.; Kennedy, A. R.; O'Hara, C. T. Exploring the Solid State and Solution Structural Chemistry of the Utility Amide Potassium Hexamethyldisilazide (KHMDS). *Dalton Trans.* **2017**, *46*, 6392.
(45) (a) Klinkhammer, K. W.; Klett, J.; Xiong, Y.; Yao, S. Homo- and Heteroleptic Hypersilylcuprates — Valuable Reagents for the Synthesis of Molecular Compounds with a Cu-Si Bond. *Eur. J. Inorg. Chem.* **2003**, *2003*, 3417. (b) Schumann, H.; Hummert, M.; Lukoyanov, A. N.; Fedushkin, I. L. Sodium Cation Migration Above the Diimine pi-System of Solvent Coordinated dpp-BIAN Sodium Aluminum Complexes (dpp-BIAN = 1,2-Bis[(2,6-diisopropylphenyl)imino]acenaphthene). *Chem.—Eur. J.* **2007**, *13*, 4216.
(46) Morita, H.; Van Beylen, M. New Vistas on the Anionic Polymerization of Styrene in Non-Polar Solvents by Means of Density Functional Theory. *Polymers* **2016**, *8*, 371.
(47) Gutmann, V. *The Donor-Acceptor Approach to Molecular Interactions*; Plenum: New York, 1978.
(48) (a) Seligson, A. L.; Trogler, W. C. Cone Angles for Amine Ligands. X-ray Crystal Structures and Equilibrium Measurements for Ammonia, Ethylamine, Diethylamine, and Triethylamine Complexes with the [bis(Dimethylphosphino)ethane]methylpalladium(II) Cation. *J. Am. Chem. Soc.* **1991**, *113*, 2520. (b) Choi, M.-G.; Brown, T. L. A Molecular Mechanics Model of Ligand Effects. 4. Binding of Amines to Chromium Pentacarbonyl: ER Values for Amines. *Inorg. Chem.* **1993**, *32*, 1548. (c) Widenhoefer, R. A.; Buchwald, S. L. Formation of Palladium Bis(amine) Complexes from Reaction of Amine with Palladium Tris(o-tolyl)phosphine Mono(amine) Complexes. *Organometallics* **1996**, *15*, 3534.
(49) Zhang, Z.; Collum, D. B. Structures and Reactivities of Sodiated Evans Enolates: Role of Solvation and Mixed Aggregation on the Stereochemistry and Mechanism of Alkylations. *J. Am. Chem. Soc.* **2019**, *141*, 388.
(50) (a) Jarek, R. L.; Denson, S. C.; Shin, S. K. Solvation of the Li^+-Cl^--Li^+ Triple Ion in the Gas Phase. *J. Chem. Phys.* **1998**, *109*, 4258. (b) Chapman, D. M.; Hester, R. E. Ab Initio Conformational Analysis of 1,4-Dioxane. *J. Phys. Chem. A* **1997**, *101*, 3382.
(51) (a) Kaga, A.; Hayashi, H.; Hakamata, H.; Oi, M.; Uchiyama, M.; Takita, R.; Chiba, S. Nucleophilic Amination of Methoxy Arenes Promoted by a Sodium Hydride/Iodide Composite. *Angew. Chem., Int. Ed.* **2017**, *56*, 11807. (b) Pang, J. H.; Ong, D. Y.; Watanabe, K.; Takita, R.; Chiba, S. Leaving Group Ability in Nucleophilic Aromatic Amination by Sodium Hydride-Lithium Iodide Composite. *Synthesis* **2020**, *52*, 393.
(52) (a) Pang, J. H.; Kaga, A.; Roediger, S.; Lin, M. T.; Chiba, S. Revisiting the Chichibabin Reaction: C2 Amination of Pyridines with a NaH-Iodide Composite. *Asian J. Org. Chem.* **2019**, *8*, 1058. (b) Ezquerra, J.; Alvarez-Builla. J. Org. Sonochem. A Facile Synthesis of 1-Methylisoquinoline. *Org. Prep. Proced. Int.* **1985**, *17*, 190. (c) Pang, J. H.; Kaga, A.; Chiba, S. Nucleophilic Amination of Methoxypyridines by a Sodium Hydride-Iodide Composite. *Chem. Commun.* **2018**, *54*, 10324. (d) Narayan, S.; Seelhammer, T.; Gawley, R. E. Microwave-Assisted Solvent-Free Amination of Halo-(Pyridine or Pyrimidine) without Transition Metal Catalyst. *Tetrahedron Lett.* **2004**, *45*, 757. (e) Garia, A.; Jain, N. Transition-Metal-Free Synthesis of Fused Quinazolinones by Oxidative Cyclization of N-Pyridylindoles. *J. Org. Chem.* **2019**, *84*, 9661.
(53) Oliveri, I. P.; Maccarrone, G.; Di Bella, S. A Lewis Basicity Scale in Dichloromethane for Amines and Common Nonprotogenic Solvents Using a Zinc(II) Schiff-Base Complex as Reference Lewis Acid. *J. Org. Chem.* **2011**, *76*, 8879.
(54) Chakrabarti, P.; Dunitz, J. D. Directional Preferences of Ether O-Atoms Towards Alkali and Alkaline Earth Cations. *Helv. Chim. Acta* **1982**, *65*, 1482.
(55) (a) *Polyamine-Chelated Alkali Metal Compounds*; Langer, A. W., Jr., Ed.; American Chemical Society: Washington, DC, 1974. (b) Collum, D. B. Is *N,N,N′,N′*-Tetramethylethylenediamine a Good Ligand for Lithium? *Acc. Chem. Res.* **1992**, *25*, 448.
(56) Bauer, W.; Schleyer, P. v. R. *Advances in Carbanion Chemistry*; Snieckus, V., ed.; JAI: New York, 1992; p 89.
(57) Pratt, L. M.; Mogali, S.; Glinton, K. Solvent Effects on the Aggregation State of Lithium Dialkylaminoborohydrides. *J. Org. Chem.* **2003**, *68*, 6484.
(58) (a) Cabello, N.; Kizirian, J. C.; Alexakis, A. Enantioselective Addition of Aryllithium Reagents to Aromatic Imines Mediated by 1,2-Diamine Ligands. *Tetrahedron Lett.* **2004**, *45*, 4639. (b) Mealy, M. J.; Luderer, M. R.; Bailey, W. F.; Sommer, M. B. Effect of Ligand Structure on the Asymmetric Cyclization of Achiral Olefinic Organolithiums. *J. Org. Chem.* **2004**, *69*, 6042. (c) Cointeaux, L.; Alexakis, A. Enantioselective Addition of Organolithium Reagents to Quinoline Catalyzed by 1,2-Diamines. *Tetrahedron: Asymmetry* **2005**, *16*, 925. (d) Kizirian, J. C.; Cabello, N.; Pinchard, L.; Caille, J. C.; Alexakis, A. Enantioselective Addition of Methyllithium to Aromatic Imines Catalyzed by C_2 Symmetric Tertiary Diamines. *Tetrahedron* **2005**, *61*, 8939.
(59) Van Leeuwen, P. W. N. M.; Kamer, P. C. J.; Reek, J. N. H.; Dierkes, P. Ligand Bite Angle Effects in Metal-Catalyzed C-C Bond Formation. *Chem. Rev.* **2000**, *100*, 2741.
(60) (−)-Sparteine. Hoppe, D.; Morgan, B. J.; Kozlowski, M. C. In *Encyclopedia of Reagents for Organic Synthesis*; John Wiley & Sons, Ltd.: Chichester, UK, 2007; pp 1−6.
(61) Garcia-Alvarez, P.; Kennedy, A. R.; O'Hara, C. T.; Reilly, K.; Robertson, G. M. Synthesis and Structural Chemistry of Alkali Metal tris(HMDS) Magnesiates Containing Chiral Diamine Donor Ligands. *Dalton Trans.* **2011**, *40*, 5332.
(62) (a) Tian, Z.; Fattahi, A.; Lis, L.; Kass, S. R. Neutral Intramolecular Hydrogen-Bonded Bases. *Croat. Chem. Acta.* **2009**, *82*, 41. (b) Maksić, Z. B.; Kovačević, B.; Vianello, R. Advances in Determining the Absolute Proton Affinities of Neutral Organic Molecules in the Gas Phase and Their Interpretation: A Theoretical Account. *Chem. Rev.* **2012**, *112*, 5240.
(63) Lannert, K. P.; Joesten, M. D. Metal Complexes of Nonamethylimidodiphosphoramide. *Inorg. Chem.* **1968**, *7*, 2048. (b) Bokolo, K.; Delpuech, J. J.; Rodehüser, L.; Rubini, P.; Courtois, A.; Elkaim, E.; Protas, J.; Rinaldi, D. Conformations of the Nonbonded and the Coordinated Ligand Nonamethylimidodiphosphoramide (NIPA) in the Solid State and in Solution. X-Ray Structure Determinations, NMR Study, and Theoretical Calculations on the NIPA Molecule and the Complex $[UO_2(NIPA)_2C_2H$. *J. Am. Chem. Soc.* **1984**, *106*, 6333.
(64) Collum, D. B.; Cho, B. unpublished.
(65) (a) Rodehuser, L.; Chniber, T.; Rubini, P.; Delpuech, J. J. Mixed Ligand Complexes Containing *β*-diphosphoramides. I.

https://dx.doi.org/10.1021/acs.joc.0c02546
J. Org. Chem. 2021, 86, 2406−2422

Substitution of DMSO by NIPA in Solvates of Cadmium(II). A Cadmium-113 NMR Study. *Inorg. Chim. Acta* **1988**, *148*, 227. (b) Tomoi, M.; Onozawa, T.; Seki, K.; Kakiuchi, H. Anionic Polymerization of Vinyl Monomers with Organometallic Compound—Phosphoramide System. *Polym. J.* **1975**, *7*, 372.

(66) (a) Rubini, P. R.; Rodenhueser, L.; Delpuech, J. J. A Nuclear Magnetic Resonance Study of Metal Complexes of Nonamethylimidodiphosphoramide. *Inorg. Chem.* **1979**, *18*, 2962.

(67) Cossentini, M.; Strzalko, T.; Seyden-Penne, J. A Study of the Michael Reaction in the Presence of Complexing Agents for Alkali Metal Cations in Aprotic Media or Under Phase-Transfer Conditions. *Bull. Soc. Chim. France* **1987**, 531.

(68) Delville, A.; Detellier, C.; Gerstmans, A.; Laszlo, P. Preferential Solvation of the Sodium Cation in Binary Mixtures of Tetrahydrofuran with Polyamines, in Relation with the Chelate Effect. *Helv. Chim. Acta* **1981**, *64*, 556.

(69) Fraenkel, G.; Subramanian, S.; Chow, A. The Carbon-Lithium Bond in Monomeric Aryllithiums: Dynamics of Exchange, Relaxation, and Rotation. *J. Am. Chem. Soc.* **1995**, *117*, 6300.

(70) Crown−sodium−solvent complexes are prevalent in the crystallographic literature. While there are a couple of THF/15-crown-5 complexes in the Cambridge Database, donor solvent/18-crown-6 complexes are commonplace. No evidence for 12-crown-4 mixed solvates could be found. (a) Campazzi, E.; Solari, E.; Scopelliti, R.; Floriani, C. Lanthanide Organometallic Chemistry Based on the Porphyrinogen Skeleton: Acetylene and Ethylene Bridging Praseodymium and Neodymium H5:H1:H5:H1-Bonded to Meso-Octaethylporphyrinogen. *Chem. Commun.* **1999**, *17*, 1617. (b) Uhl, W.; Hannemann, F. A Methylene Bridged Dialuminium Compound as a Chelating Lewis Acid - Complexation of Azide and Acetate Anions by $R_2Al\text{-}CH_2\text{-}AlR_2$ [R = $CH(SiMe_3)_2$]. *J. Organomet. Chem.* **1999**, *579*, 18. (c) Hervé, A.; Thuéry, P.; Ephritikhine, M.; Berthet, J. C. Structural Diversity in Cyanido Thorocene Complexes. *Organometallics* **2014**, *33*, 2088. (d) Cambillau, C.; Bram, G.; Corset, J.; Riche, C. Complexes Formés Par Addition d'éthers-Couronnes Aux Énolates de Na^+ et K^+ de l'Acétylacétate d'éthyle: Structures Cristallines et Système d'équilibres En Solution Dans le THF et le DMSO. *Can. J. Chem.* **1982**, *60*, 2554.

(71) Titrating a solution of NaHMDS in toluene or MTBE with two ligands (two crowns, for example) will necessarily produce solvates of *both* at up to 0.5 equiv of each. Only when an excess has been added can the preference be established. The protocol is expedient, and the low concentrations serve as control experiments.

(72) (a) Soula, G. Tris(polyoxaalkyl)amines (Trident), a New Class of Solid-Liquid Phase-Transfer Catalysts. *J. Org. Chem.* **1985**, *50*, 3717. (b) Starks, C. M.; Liotta, C. L.; Halpern, M. *Phase-Transfer Catalysis*; Chapman & Hall: New York, 1994.

(73) Xu, M.; Jupp, A. R.; Qu, Z. W.; Stephan, D. W. *Angew. Chem., Int. Ed.* **2018**, *57*, 11050.

(74) Wang, Y.; Song, S.; Xu, C.; Hu, N.; Molenda, J.; Lu, L. Development of Solid-State Electrolytes for Sodium-Ion Battery-A Short Review. *NMS* **2019**, *1*, 91.

(75) There are an enormous number of documented $^+Na(THF)_6$ and $^+Na(\kappa^2\text{-DME})_3$ gegenions. For an example of both, see: Livingstone, Z.; Hernan-Gomez, A.; Baillie, S. E.; Armstrong, D. R.; Carrella, L. M.; Clegg, W.; Harrington, R. W.; Kennedy, A. R.; Rentschler, E.; Hevia, E. *J. Chem. Soc., Dalton Trans.* **2016**, *45*, 6175.

(76) For a particularly incisive comparison of methods for calculating alkali metal solvation using both explicit and continuum models of solvation (including lithium and sodium solvated by THF and DME), see: Ziegler, M. J.; Madura, J. D. Solvation of Metal Cations in Non-aqueous Liquids. *J. Solution Chem.* **2011**, *40*, 1383.

(77) Review of ^{19}F NMR spectroscopy in organometallic chemistry: Espinet, P.; Albeniz, A. C.; Casares, J. A.; Martinez-Ilarduya, J. M. ^{19}F NMR in Organometallic Chemistry: Applications of Fluorinated Aryls. *Coord. Chem. Rev.* **2008**, *252*, 2180.

(78) Excluding the explicitly silicon-centric world of organosilicon chemistry, one finds remarkably few instances in which ^{29}Si NMR spectroscopy is used by the general organic chemistry community, and most are mechanistic studies. Applications in synthesis include: (a) Wu, N.; Wahl, B.; Woodward, S.; Lewis, W. 1,4-Addition of $TMSCCl_3$ to Nitroalkenes: Efficient Reaction Conditions and Mechanistic Understanding. *Chem. - Eur. J.* **2014**, *20*, 7718. (b) Humbrias-Martin, J.; Perez-Aguilar, M. C.; Mas-Balleste, R.; Dentoni Litta, A.; Lattanzi, A.; Della Sala, G.; Fernandez-Salas, J. A.; Aleman, J. Enantioselective Conjugate Azidation of α,β-Unsaturated Ketones Under Bifunctional Organocatalysis by Direct Activation of $TMSN_3$. *Adv. Synth. Catal.* **2019**, *361*, 4790. (c) Kolomeitsev, A.; Bissky, G.; Lork, E.; Movchun, V.; Rusanov, E.; Kirsch, P.; Röschenthaler, G.-V. Different Fluoride Anion Sources and (Trifluoromethyl)trimethylsilane: Molecular Structure of Tris(dimethylamino)sulfonium Bis(trifluoromethyl)trimethylsiliconate, the First Isolated Pentacoordinate Silicon Species with Five Si-C bonds. *Chem. Commun.* **1999**, 1017. (d) Maggiarosa, N.; Tyrra, W.; Naumann, D.; Kirij, N. V.; Yagupolskii, Y. L. $[Me_3Si(CF_3)F]^-$ and $[Me_3Si(CF_3)_2]^-$: Reactive Intermediates in Fluoride-Initiated Trifluoromethylation with Me_3SiCF_3 An NMR Study. *Angew. Chem., Int. Ed.* **1999**, *38*, 2252. (e) Kobayashi, S.; Nishio, K. Facile and Highly Stereoselective Allylation of Aldehydes Using Allyltrichlorosilanes in DMF. *Tetrahedron Lett.* **1993**, *34*, 3453. (f) Denmark, S. E.; Barsanti, P. A.; Beutner, G. L.; Wilson, T. W. Enantioselective Ring Opening of Epoxides with Silicon Tetrachloride in the Presence of a Chiral Lewis Base. Mechanism Studies. *Adv. Synth. Catal.* **2007**, *349*, 567. (g) Denmark, S. E.; Eklov, B. M. Neutral and Cationic Phosphoramide Adducts of Silicon Tetrachloride: Synthesis and Characterization of Their Solution and Solid-State Structures. *Chem. - Eur. J.* **2008**, *14*, 234. (h) Bobbink, F. D.; Menoud, F.; Dyson, P. J. Synthesis of Methanol and Diols from CO_2 via Cyclic Carbonates Under Metal-Free, Ambient Pressure, and Solvent-Free Conditions. *ACS Sustainable Chem. Eng.* **2018**, *6*, 12119.

https://dx.doi.org/10.1021/acs.joc.0c02546
J. Org. Chem. 2021, 86, 2406−2422